1 **Alpine gullies system evolution: Erosion drivers and control factors. Two**

2 **examples from the western Italian Alps**

3

4 Bollati I.M.[(1,\*)], Masseroli A.[(1)], Mortara G.[(2)], Pelfini M.[(1)], Trombino L.[(1)]

5

6 Università degli Studi di Milano, Milano, Italia

7 Via Mangiagalli, 34 - 20133 Milan

8 irene.bollati@unimi.it

9 anna.masseroli@unimi.ti

10 manuela.pelfini@unimi.it

11 luca.trombino@unimi.it

12 (2) CNR –IRPI - Istituto di Ricerca per la Protezione Idrogeologica

13 Strada delle Cacce, 73 10135 – Torino

14 giovanni.mortara@irpi.cnr.it

15

16 (\*) Corresponding Author: irene.bollati@unimi.it

17 Tel.: +390250315516

18 Fax: +390250315494

19

20 **Abstract**

21 Denudation processes affecting mountain slopes may vary according to different

22 factors (e.g., lithology and structural setting of bedrock, climate, relief features),

23 which may be very diverse at the local scale. Gully complex systems, characterised by

24 morphological features similar to those developing in other climate contexts (i.e.,

25 pseudo-badlands) are also becoming common at higher altitudes and latitudes. The

1

26    selected study cases of Gran Gorgia (Susa Valley) and Saint Nicolas (Aosta Valley),

27    in the Western Italian Alps, are sites of geomorphological interest as they are

28    specifically relevant for their scientific features. The aims of this work are (i)

29    reconstructing the morphometric evolution of gullies edges and vegetation

30    colonisation in specific years by means of multitemporal spatial analysis on variation

31    of surface areas affected by erosion; (ii) performing dendrogeomorphological analysis

32    to spatially reconstruct, with a more continuous record through time, the effects of

33    denudation processes affecting trees colonising the different regions of the gullies and

34    the erosion rates by using dendrogeomorphological indicators (i.e., compression

35    wood, traumatic resin ducts) and exposed roots and (iii) performing geopedological

36    investigations aimed at deriving data on aggradation/degradation episodes along the

37    slopes surrounding such hot-spots of erosion through time. Multidisciplinary analyses

38    regarding the study sites allowed for detailing of erosional history of the studied

39    slopes detecting the prevailing drivers of their evolution. According to the results and

40    considering the common climate and bedrock conditions, the structural background

41    seems to have more influence on slope evolution at the Saint Nicolas site, while

42    superficial geomorphic processes seem to be more relevant at the Gran Gorgia site.

43    Because the sites have already been recognised as part of geoheritage by local

44    authorities, the data obtained in the present research on their genesis, evolution, and

45    local drivers affecting the rates of denudation (i.e., scientific relevance of the site)

46    suggests that description of the sites for dissemination purposes should include links

47    to the entire slope history.

48

49    *Keywords*: gully systems; morphometry; dendrogeomorphology; geopedology;

50    denudation rates; western Italian Alps

51

**1. Introduction**

53

Denudation processes affecting mountain slopes are variable in intensity according to

different factors. Lithology and structural setting of bedrock (Cossart et al., 2013), as

well as climate and relief features (Della Seta et al., 2009), are among the most

efficient drivers and are very diversified at the local scale (Keiler et al., 2010).

In the context of mass wasting, gully systems are considered hot-spots of erosion in

different morphoclimatic environments (Della Seta et al., 2009; Bollati et al., 2016a).

The most studied cases are located in Mediterranean-like climate conditions, where

dry periods are frequently followed by intense rainfall and where such sequence of

meteorological conditions triggers the principal erosion events and contributes to the

genesis of iconic landscapes (i.e., badlands like the Italian *calanchi* and *biancane*;

Della Seta et al., 2009; Bollati et al., 2016b).

Morphological features similar to the badlands and gully systems developing in the

Mediterranean climate are also becoming common at higher altitudes and latitudes

(i.e., *pseudo-badlands sensu* Bollati et al., 2017). At higher altitudes, gullies mainly

develop on loose glacial deposits, for example, on the inner flanks of lateral moraines,

as a consequence of water runoff following deglaciation (e.g., Curry, 1999;

Ballantyne, 2002; Cossart and Fort, 2008). This is a typical *paraglacial* readjustment

affecting deglaciated areas, as described by Mercier et al. (2009). In polar

environments, the *Index of gullying* on sediment mantled slopes has been in fact

proposed by the authors for providing a time constraint to deglaciation in an area.

According to Curry (1999) and Bollati et al. (2017), erosion rates affecting glacial

deposits in mountain areas decrease proportionally to deglaciation time, proceeding

3

76 toward downvalley (Ballantyne, 2002), taking into account the local conditions

77 (Cossart and Fort, 2008).

78 Besides progressive and continuous erosional work affecting mountain ranges at

79 regional scale (e.g., Hinderer, 2001), locally the sudden evacuation of a huge amount

80 of debris during single meteorological events can generate new landforms (Chiarle

81 and Mortara, 2001). Extreme heavy rainfall events are becoming even more common

82 within the ongoing climate conditions (Frei et al., 1998). After such perturbations

83 (Ballantyne, 2002; Cossart and Fort, 2008), new landscape features may evolve under

84 routine conditions recovering more regular erosion rates.

85 In addition to specific climatic and weather conditions, lithology and structural

86 bedrock settings significantly contribute to the genesis of these erosional landforms,

87 especially in tectonically active mountain ranges (e.g., *calanchi*; Farifteh and Soeters,

88 2006). Lithological and structural controls on the geomorphological dynamic along

89 slopes play a key role at different spatial and time scales (Fort, 2000). Slopes

90 characterised by tectonically deformed lithotypes present, as common features, deep-

91 seated gravitational slope deformations (DSGSDs; Mortara and Sorzana, 1987). These

92 DSGSD periodical reactivations may induce intensification of mass wasting and water

93 erosion processes along the weaker portion of slopes (Mortara and Sorzana, 1987, and

94 references therein). These deep deformations may severely affect the hydrographic

95 patterns (Galeandro et al., 2013) until the complete obliteration of the stream network

96 (Korup, 2005), inducing changes in water erosional patterns.

97 Iconic examples of gullies or overincision systems are locally evident in the Alpine

98 range. Gully systems are locally characterised along their inner flanks by the

99 development of, more or less pervasive, pseudo-badland features (Bollati et al., 2017;

100 Fig. 1). As mentioned before, these deep gullies are sometimes consequent to single

4

101    extreme meteorological events, which have affected glacial deposits in more or less

102    recent times (Mortara et al., 1995; Chiarle and Mortara, 2001; Chiarle et al., 2007).

103    The gully systems in Alpine contexts can be grouped into three main categories, as

104    used in this paper, according to the age of the deposits affected by rill erosion, to the

105    rates of denudation, and finally, to the degree of vegetation colonisation. Gully

106    systems developed on glacial deposits dating to the Little Ice Age (LIA) and, more

107    frequently, to even more recent glacial stages (category 1; Fig. 1A) are reported as the

108    most meaningful cases. Breaches may occur in moraines, and an impressive mass

109    wasting (mainly debris flow) may occur, especially during extreme meteorological

110    events. These landforms are usually still *fresh*, located at higher altitudes, not

111    colonised by arboreal vegetation and characterised by incipient soils. Some examples

112    for the Italian Alps are reported in the literature (e.g., Chiarle and Mortara, 2001;

113    Chiarle et al., 2007): (i) the Sissone Glacier moraine system (Valmalenco; central

114    Italian Alps) reworked by a disastrous event that occurred on 15 September 1950,

115    with an estimated sediment delivery $> 1 \times 10^6$ m$^3$ (Chiarle et al., 2007); (ii) the

116    Mulinet Glacier moraine system (Valle di Lanzo, western Italian Alps; Fig. 1A) where

117    the overincision of the moraine occurred on 29 September 1993, inducing an

118    estimated sediment delivery of $0.8 \times 10^6$ m$^3$ (Mortara et al., 1995; Fig. 1A).

119    The second type of incisions affects older glacial deposits, related to upper

120    Pleistocene. This typology is generally located at lower altitudes or several kilometres

121    away from the current glacial snout position (category 2; Fig. 1C). In these cases,

122    plant and tree colonisation of the bare surface is driven by both natural and human

123    factors, soils are more developed and erosion rates are expected to be lower (Curry,

124    1999; Bollati et al., 2017). Some examples in the Italian Alps are represented by (i)

5

125 Saint Nicolas *calanchi* (Aosta Valley, western Italian Alps; Fig. 1C); ii) Neraissa

126 Basins (Valle di Stura di Demonte, western Italian Alps).

127 Intermediate categories with transitional features between the two previous categories

128 also exist (category 3; Fig. 1B) and an example is represented by the Gran Gorgia

129 (Susa Valley, western Italian Alps; Fig. 1B).

130 Categories 2 and 3 are often located along the flank of the main Alpine valleys that

131 underwent upper Pleistocene glacial modelling (e.g., Balteo Glacier for Saint Nicolas

132 calanchi; Susa Glacier for Gran Gorgia). Following deglaciation, these valley slopes

133 were locally affected by different postglacial processes such as decompression along

134 preferential directions (e.g., debutressing; Cruden and Hu, 1993) according to local

135 geological, structural and geomorphological conditions (e.g., DSGSDs); this may

136 have different fallouts on the sediment cascade fluxes (McColl et al., 2012; Cossart et

137 al., 2013).

138 The importance of such sites in understanding the post-glacial evolution of mountain

139 landscapes, considering all the interplaying factors, opens the possibility of discussing

140 the meaning of the most representative landforms like *geosites* or *sites of geological*

141 *interest* (*sensu* Wimbledon, 1999). According to the definition by Wimbledon (1999),

142 they represent key sites, characterised by a high scientific value, important for

143 detecting the main stages of Earth system evolution. Moreover, gully systems are

144 particularly meaningful from an educational point of view (Bollati et al., 2016a;

145 Zgłobicki et al., 2017). They are *sites of geomorphological interest* or *geomorphosites*

146 (*sensu* Panizza, 2001) and according to the classification proposed by Pelfini and

147 Bollati (2014), they may be categorised as *active geomorphosites* or *evolving passive*

148 *geomorphosites* depending on the type of the processes currently affecting the sites. In

149 the first case, gully systems as geomorphosites are still evolving caused by their own

6

150    genetic process (i.e., badlands systems); in the second case, the processes inducing

151    morphological changes are different from the genetic ones (i.e., pseudo-badlands

152    superimposing on moraines). Hence, besides their scenic value that usually represents

153    the main motor for raising public interest, the scientific value of these landforms

154    should be central and requires even further investigations (Reynard et al., 2007;

155    Brilha, 2016).

156    If the events responsible for the genesis and/or for the morphological changes of

157    gullies in category 1 are well documented in the historical archives, less details are

158    available for categories 2 or 3 developed on older deposits (Chiarle and Mortara,

159    2001): so research on their evolution and respective drivers can be very important for

160    the reasons previously exposed. For this purpose, two sites were selected as study

161    cases: the Gran Gorgia (Fig. 1B; site A in Fig. 2) and the Saint Nicolas calanchi (Fig.

162    1C; sites B1 and B2 in Fig. 2).

163    Multidisciplinary approaches have been described in the literature (e.g., Mercier et al.,

164    2009; Burga et al., 2010; Compostella et al., 2013; Pelfini et al., 2014; Bollati et al.,

165    2016a; Eichel et al., 2016) as the best way to detect the contribution of multiple

166    factors (i.e., lithology and tectonic setting of bedrock, climate), which may drive

167    geomorphic processes like water erosion. A multidisciplinary approach could allow

168    for filling the gaps in the results obtained, operating using one kind of analysis to

169    confirm other deriving results.

170    In the present paper we aim at: (i) reconstructing the morphometric evolution of gully

171    systems and vegetation colonisation time by means of multitemporal spatial analysis

172    on surface morphological changes under water erosion; (ii) reconstructing in detail,

173    through dendrogeomorphological analysis, the progressive spatial surface denudation

174    and changes in erosion rates, by analysing trees and exposed roots and using different

175     indicators (i.e., compression wood, traumatic resin ducts); (iii) obtaining data on

176     successive aggradation/degradation episodes along slopes surrounding such hotspots

177     through geopedological investigations; and (iv) identifying which control factors exert

178     a predominant role on denudation patterns in such contexts.

179

180     **2. Study areas**

181

182     The study sites are located in the western Italian Alps (Fig. 2) at the local altitude of

183     the treeline ecotone. Their distinctive traits are described in the following sections.

184     Both represent key sites for investigating gully erosion and for assessing their role as

185     components of the regional geoheritage, as documented by their occurrence within

186     local and national geosite catalogues.

187

188     *2.1. Gran Gorgia (Susa Valley; Fig. 1B; site A in Fig. 2)*

189     The Gran Gorgia gully (GG) is located on the northern side of the lower Susa Valley

190     in the Chianocco Municipality (Turin Province). The slope is characterised by the

191     outcrop of rocks belonging to two main tectonometamorphic units (Cadoppi et al.,

192     2002). The Piedmont Zone (PZ) oceanic units and, locally, the *Val di Susa-Valle di*

193     *Lanzo-Monte Orsiera tectonometamorphic unit* (SU), constitute the water divide

194     between the Susa and Lanzo valleys. The main lithologies of the SU are serpentinites

195     and serpenitoschists, prasinites, and metasedimentary rocks like calcschists. The SU

196     overthrusts the *Dora-Maira tectonometamorphic unit* (DM), representing the

197     Mesozoic continental margin units included in the Middle Penninic. Locally the

198     dolomitic marbles of the Foresto-Chianocco-Mt. Molaras Complex constitutes the

199     DM. The tectonic contact between SU and DM, marked by a very evident marble

200  bank, corresponds to the current head of the GG gully. According to Mortara (1975),

201  the marble rocky outcrop may represent an obstacle for the regressive evolution of the

202  gully.

203  The lithostructural control is relevant along the Susa Valley; and it is documented,

204  especially on the southern side, by several DSGSDs (Cadoppi et al., 2007).

205  The GG gully develops NNW-SSE. It is located in the source area of the Prebec

206  streams and it is incised in the upper Pleistocene glacial deposits (undistinguished till)

207  pertinent to the tributary basin of the main valley, which is drained by the Dora

208  Riparia and shaped, in ancient times, by the Susa Glacier (Sacco, 1921; Cadoppi et

209  al., 2002; Ivy-Ochs et al., 2018). The Dora Riparia Valley outlet, near the town of

210  Torino and about 40 km away from the GG area, is characterised by the presence of

211  the Rivoli-Avigliana morainic amphitheatre, one of the most important and intact

212  witnesses of the Pleistocene glacial advances as far as the Po Plain (Lucchesi et al.,

213  2015; Giardino et al., 2017; Ivy-Ochs et al., 2018). The glacial deposits related to the

214  Prebec tributary basin span between 1000 and 1850 m asl (Cadoppi et al., 2002). At

215  this altitude tributary glaciers flow into the main glacial basin belonging to the Susa

216  Valley. The slopes surrounding the GG gully are currently affected by water and

217  gravity-related processes (rock degradation and falls, landslides and debris flows) and

218  by snow avalanches with the associated deposits. Locally, elongated ridges are

219  present, interpreted by Sacco (1921) as deriving from ice-snow field deposits and,

220  more recently, related with combined snow and gravity activity (Cadoppi et al., 2002).

221  The GG is characterised by an asymmetric shape with the eastern slope longer and

222  less steep, with a more elevated upper edge than the western one. Inner slopes are

223  characterised by parallel linear ridges and gullies. The scarp edges are irregular,

224  according to the prevailing geomorphic process: (i) water runoff where slope

225  steepness is lower and (ii) debris fall (i.e., coarse boulder) where steepness increases

226  until the vertical. The eastern edge is interrupted by a breach generated by regressive

227  erosion acting on the western slope of the eastward adjacent valley.

228  The genesis of the GG, whose presence has been slightly perceptible at least since the

229  early twentieth century on historical topographic maps, was hypothesised to be related

230  with a single extreme meteorological event that occurred during the fifteenth century

231  (Regione Piemonte, 1995). The hypothesis is supported by the morphological

232  analogies with the breach in the Mulinet Glacier moraine in 1993 (Fig. 1, A; Chiarle

233  and Mortara, 2001). The volume of eroded sediment during the single event is about

234  $1.5 \times 10^6 \, m^3$ (Aigotti et al., 2004).

235  According to Mortara (1975), the Prebec basin has undergone an average of 1600

236  flood events during the last 10,000 years. The author estimated a total amount of $80 \times$

237  $10^6 \, m^3$ of delivered sediment, representing almost the totality of the volume of the

238  alluvial fan on which the Chianocco village is built. Several recent hydrogeological

239  instability events affected the Prebec basin (e.g., June 1957, August 1977 and 1978,

240  November 1994, October 2000, August 2002; Tropeano et al., 1999, 2006). A debris

241  mass of $0.05 \times 10^6 \, m^3$ was deposited on the Chianocco alluvial fan during one of the

242  most disastrous events that occurred on 12-16 June 1957 (Mortara, 1975). In other

243  cases, the debris floods also affected touristic infrastructures (camping), as on 14

244  August 1978 (Mortara and Turitto, 1989). If several damages affected the village and

245  the surrounding areas in the historical records of events, many human interventions

246  also stabilised the stream (i.e., weirs) and the adjacent slopes (i.e., reforestation)

247  (Anselmo et al., 1975; Mortara, 1975).

248  In this area, as a consequence of slope steepness and of the presence of surficial

249  erosion caused by water-driven processes, only soils rich in coarse material and

10

250 poorly developed and only in a few cases with a surface layer rich in organic matter

251 are present. In fact, Entisols and Inceptisols are the most common soil types in the GG

252 study area (Carta dei Suoli del Piemonte, 1:25.000; IPLA, 2007).

253 Concerning climate, the Susa Valley, elongated in the E-W direction, is one of the

254 most drought-affected valleys of the western Italian Alps (De Luca et al., 2009),

255 similar to the climate of the Italian southern Alps region. According to the data from

256 the Prarotto weather station (1440 m asl) (Arpa Piemonte,

257 http://www.arpa.piemonte.gov.it/), local climate conditions, related to the period

258 1998-2014 (excluding the years 2004, 2006, and 2013), are characterised by mean

259 annual rainfalls of 848 mm. Mean annual temperatures for the period 1998-2017

260 (excluding the years 2004, 2013, and 2014) vary between the minimum average

261 values recorded in January (-0.1°C) and the maximum average values recorded in July

262 (15.9°C). The temperature annual range at 1440 m a.s.l is ~ 16°C.

263 The site has relations with the Rivoli-Avigliana morainic amphitheatre geosite

264 (Lucchesi et al., 2015; Giardino et al., 2017) and is located on a slope along the Susa

265 Valley. In addition, Giordano et al. (2016) reconsidered the Franks trail, developing

266 along the Susa Valley and along which the site is located, as a cultural-geological

267 path. Moreover, the site is inserted in the list of geosites of Turin Province (Aigotti et

268 al., 2004) and is reported in the ISPRA national geosites inventory

269 (http://sgi.isprambiente.it/geositiweb/scheda_geosito.aspx?id_geosito_x=1439).

270

271 *2.2. Saint Nicolas calanchi (Aosta Valley; Fig. 1C; sites B1 and B2, Fig. 2)*

272 The Saint Nicolas calanchi (SN) is a gully incision developing mainly NNW-SSE and

273 located on the northern side of the Aosta Valley in the Saint Nicolas municipality

274 (Aosta Province). The slope hosting the site is characterised by the presence of

275    tectonometamorphic units pertaining to continental and oceanic domains (Polino et

276    al., 2015). The slope is affected by the presence of the relevant DSGSD of Punta

277    Leysser (Forno et al., 2012), whose limits roughly correspond to the tectonic contacts

278    between structural units. In detail, the western and northern edge of the DSGSD are

279    characterised by the *Gran San Bernardo multinappe system*, included in the Middle

280    Pennidic domain, which is constituted by the Palaeozoic continental units of *Rutor*

281    (paragneiss and micaschists with prealpine relicts) and *Fallère-Metailler* (micaschists,

282    paragneiss, and metabasites). The central portion of the slope, where the greatest part

283    of the DSGSD is located, is dominated by the Mesozoic *Aouilletta ophiolitic unit*

284    (undistinguished calcschists, metabasites and prasinitic gneiss, serpentinites and

285    oficarbonates with local marble), representing a portion of the Piedmont Zone

286    separated from the Penninic units by the *Inner Houillere Front*. Locally, along the

287    slope, the shear and faulted zones are marked by carbonate-cemented breccia.

288    As mentioned before, the morphology of the slope is mainly affected by the activity

289    of the Punta Leysser DSGSD that produces typical traits such as trenches,

290    counterscarps, and double or multiple ridges. A particular feature is constituted by the

291    presence of travertines locally outcropping and related to water infiltration caused by

292    the DSGSD dynamics (Forno et al., 2016). According to Forno et al. (2013, 2016) and

293    Pini et al. (2013), the preservation of Quaternary deposits is favoured in such areas by

294    the irregularities of the slope, mainly elongated ridges, which favour deposition.

295    These areas, where deposition prevails, alternate with areas prone to erosion,

296    especially along the hydrographic network, whose pattern is driven by the structures.

297    The Quaternary sedimentation is, for the authors, strictly dependent from the

298    structural setting.

299   The site is located along the northern side of the main glacial Aosta Valley shaped by

300   the Balteo Glacier, which was fed locally by tributary glaciers (i.e., Clusellaz,

301   Verrogne, Gaboè, and Vetan; Forno et al., 2012). The witnesses of their presence,

302   besides the related deposits, are mainly glacial cirques, aretes, and rôche moutonnée,

303   as well as overdeepenings and depressions that interplay with the structurally derived

304   ones. Besides, the study site is located along the northern slope bordering the *Conca*

305   *di Aosta*, where an overdeepening was generated by the interaction between the

306   gravitational deformation and the Balteo Glacier action, allowing for the formation

307   and deposition of a great quantity of debris. Along the investigated slope, the *Ivrea*

308   *Synthem* deposits represent the witness of the last glaciation that reached the position

309   of the Ivrea morainic amphitheatre about 90 km downstream (Fig. 2) (Gianotti et al.,

310   2015). This represented, as did the Rivoli-Avigliana morainic amphitheatre, a

311   significant witness of the Pleistocene glacial advances (Lucchesi et al., 2015;

312   Giardino et al., 2017). Locally, during the Last Glacial Maximum (29-19 ky BP;

313   Gianotti et al., 2015), the Balteo Glacier reached a maximum altitude of 1800 m asl

314   (Sacco, 1927; Forno et al., 2012). In the area, within the Ivrea Synthem, the *Colle San*

315   *Carlo* and the *Excenex Subsynthems* are reported (upper Pleistocene; Polino et al.,

316   2015). The first one, constituted mainly by undistinguished till, characterises higher

317   altitudes (as far as about 2000 m asl); while the second one, essentially made by

318   locally stratified lodgement till, occupies the lower portion of the slope (as far as

319   about 1500 m asl). Another more recent Subsynthem, included in the Ivrea Synthem

320   and characterising the study area, is the *Pileo Subsynthem* related to the Lateglacial

321   stage (Upper Pleistocene - Lower Holocene; Polino et al., 2015). In the study area, its

322   deposits cover the upper portion of the slope (above 2000 m asl) and are interpreted as

323   lodgement till (Polino et al., 2015). Only near the Mont Fallère water divide, where

324  the glacial cirques are present, the very recent postglacial deposits, belonging to the

325  *Miage Synthem* (Holocene - Present), are described in the literature. Besides the

326  glacial deposits, gravity related deposits are also present.

327  Gullies represent a common feature along the slope, where the cutting of glacial

328  deposits is more evident. Gullies are more articulated and mature along the Gaboè and

329  the Montovret streams, respectively draining the geosite (at about 2000 m asl; site B1

330  in Fig. 2) and the calanchi area located to the south of Rumiod village (at about 1200

331  m asl, 3.5 km southeasterly of the geosite, site B2 in Fig. 2), while the gullies are

332  incipient in other cases. The locations of the gullies are driven by gravitational

333  morphostructures (e.g., longitudinal trenches; Forno et al., 2012). The SN geosite

334  develops upward to an abrupt westward diversion of the DSGSD western edge, along

335  the Gaboè stream. The Montovret site presents a one-sided pseudo-badlands slope,

336  west oriented, located in the core of the DSGSD. Measurements of erosion were

337  performed along the Gaboè and the Montovret gullied stream sites in the present

338  research. The SN is characterised by irregular scarp edges where water runoff or

339  gravity may prevail; and it is divided into subbasins, some of which are characterised

340  by typical badlands in a different respect to the GG site. In particular, the eastern

341  slope is more affected by gullying processes; and along the eastern scarp edge, more

342  inward with respect to the DSGSD western edge, they assume the typical morphology

343  of a 'rather small hydrographic unit, horse-shoe shaped, with a tributary system in

344  which each channel is separated from the adjacent ones by means of more or less

345  sharp ridges' (Alexander, 1980). The western edge is more regular and similar to the

346  GG, characterised by parallel ridges alternating to gullies, and is transversal with

347  respect to the main gully.

14

348    Human interventions realised in the middle of the twentieth century were addressed to

349    slow down regressive erosion by means of a series of weirs located along the Gaboè

350    stream and of reforestation practices and artificial terracing (source Regione Valle

351    D'Aosta).

352    The study area of SN is characterised by different types of soil (Carta Ecopedologica

353    d'Italia 1:250.000, 2013;

354    http://wms.pcn.minambiente.it/ogc?map=/ms_ogc/WMS_v1.3/Vettoriali/Carta_ecope

355    dologica.map). At higher altitude, thin soils (Leptosol) and soils characterised by a

356    surface layer rich in humus (Umbrisol) were mapped. Whereas, at lower altitude the

357    slope is mainly characterised by very thin and not well developed soils (Leptosol,

358    Regosol), the more stable areas are characterised by soils with weak horizon

359    differentiation, and is highlighted by changes in physical and chemical properties like

360    colour, structures or clay content (Cambisols).

361    The climate in this portion of the Aosta Valley, as in the Susa Valley elongated in the

362    E-W direction, has a semicontinental temperature regime with an annual temperature

363    range of about 20°C. Rainfall is scarce (about 680 mm in the main valley), with 70%

364    of the land receiving < 1000 mm/y (Mercalli et al., 2003). Considering the

365    meteorological trends recorded during the period 1995-2012 in Aosta (Saint

366    Christophe meteorological station; Arpa Valle d'Aosta,

367    http://cf.regione.vda.it/ufficio_idrografico.php), on average precipitation is are

368    concentrated in autumn and spring, with a minimum recorded during winter (531 mm

369    annually). Concerning temperature, the winter minimum average temperature is in

370    January (-0.4°C), and the summer maximum average temperature is in July (21.7°C),

371    with an annual thermal excursion slightly over 20°C.

372    The site is a geosite of the Aosta Valley

373    (http://www.regione.vda.it/territorio/territorio/geositi/snicolas/default_i.asp) that the

374    municipality of Saint Nicolas decided to enhance by means of a geotouristic trail

375    linking Gaboè and the Montovret calanchi sites (http://www.comune.saint-

376    nicolas.ao.it/index.php?option=com_contentandview=articleandid=183andItemid=10

377    9).

378

379    **3. Materials and methods**

380    *3.1.    Multitemporal analysis of gully surface changes caused by water and gravity*

381    *erosion*

382    The multitemporal mapping of the bare surfaces affected by water runoff (i.e.,

383    surfaces with scattered vegetation and not characterised by soil development) was

384    performed in a GIS environment (ESRI software ArcGis 10.2.1, ArcMap) using a

385    series of orthophotos available only as a GIS server of the National Web Map Service

386    (i.e., Geoportale Nazionale, WMS Service; http://wms.pcn.minambiente.it/).

387    Considering this source data, with a resolution of 0.5 m, the expected error is of $\pm 2\%$

388    (see Smiraglia et al., 2015). The orthophotos date respectively to 1989 (GG) / 1988

389    (SN); 1997 (GG and SN); 1998 (GG) / 1999 (SN); 2007 (GG) / 2006 (SN), 2012 (GG

390    and SN). After mapping the areas, percentages of surface variations during the entire

391    investigated periods were calculated with respect to the initial surface area size (i.e.,

392    1988 for SN and 1989 for GG), and the percentage of changes was also calculated for

393    each time subinterval. Additional morphometric features were derived for the GG

394    from the DTM (10 m; Regione Piemonte, http://www.geoportale.piemonte.it/cms/;

395    1997-2008) and for SN from the DTM (2 m; Regione Valle D'Aosta,

396    http://geoportale.regione.vda.it/; 2005-2008).

16

397

398    *3.2.    Dendrogeomorphological analysis*

399 Erosion caused by water runoff and slope processes (e.g., mass wasting events, snow

400 avalanches) have been investigated by means of dendrogeomorphological analyses,

401 techniques widely applied to detect, discriminate, and date geomorphic events

402 affecting trees colonising landforms (e.g., Alestalo, 1971; Guida et al., 2008; Pelfini

403 and Santilli, 2008; Stoffel and Bollschweiler, 2008).

404 In order to detect the geomorphic dynamics affecting the investigated sites and the

405 surrounding slopes, field surveys were carried out during 2013, 2015, and 2016. The

406 sampling design was established by grouping trees into subclusters ideally

407 characterised by different geomorphic dynamics and located at a progressive distance

408 from the main gully. At tree sample sites, analyses of the soil profiles were also

409 performed, where possible (see section 3.3).

410 In the GG case, 86 trees of *Larix decidua* Mill. were sampled belonging to the five

411 sub-clusters reported, in relation with soil sampling in Table 1. The total number of

412 sampled trees is 61 for the A1-A5 subclusters and 25 for the A6-A7 subclusters.

413 Along the SN slope, a similar procedure was followed. Two main sites and relative

414 subclusters were selected: the SN site along the Gaboè stream (B1) and the Rumiod

415 site along the Montovret stream (B2) (Table 1). The total number of sampled trees of

416 *Larix decidua* Mill. species is 30 for the B1.1-B1.4 subclusters and 15 for the B1.5

417 subcluster. Moreover, in the B2 area 13 trees of *Larix decidua* Mill. and 4 of *Pinus*

418 *sylvestris* L. located along the scarp edge were analysed. In both sites, a cluster of

419 undisturbed trees (at least 15 trees) was selected to build the reference chronologies to

420 be used to discriminate regional or local origin of the disturbances.

17

421    Concerning samples from the trunk, the specimens were extracted using a Pressler

422    increment borer. At least two samples in different positions for each tree were

423    extracted taking care of sampling for one core to investigate the disturbance

424    specifically (e.g., scars, tilted portion of the stem) (Stoffel and Bollschweiler, 2008).

425    Concerning the undisturbed specimens, especially those for building the reference

426    chronology, they were extracted at a standard height of 1.30 m (breast height). In

427    order to analyse root micromorphology, disks were cut using a saw.

428    After the first phase of microscopic analysis using the LINTAB system (Rinn, 1996),

429    tree ring widths were measured (accuracy of 0.01 mm) according to the features of the

430    specimen using the Lintab and TSAP systems (Rinn, 1996) and/or by means of image

431    analysis performed with WinDENDRO software (Régent Instruments Inc., 2001). The

432    mean chronologies for the disturbed and undisturbed clusters of trees were elaborated

433    by means of the cross-dating procedure with TSAP and COFECHA (Holmes et al.,

434    1986). Moreover, in order to remove growth trend, a detrending was performed by

435    means of a spline function, using Arstan (Holmes et al., 1986). Afterward, the dating

436    of each individual annual ring, and consequently disturbance, and the determination

437    of the age of geomorphic events, was possible.

438    In order to perform erosion rate estimation by means of exposed tree roots, roots were

439    the object of microscopic morphometric analysis and measurement using Lintab and

440    TSAP systems (Rinn, 1996). Roots change their micromorphology, from the

441    production of root type wood to a trunk type wood as a consequence of exposure

442    (Gärtner, 2007; Stoffel et al., 2013) (Fig. 3). According to this response of roots, the

443    erosion rates were calculated starting from the equation proposed by Hupp and Carey

444    (1990):

445                                        $E = D/A$                                        (1)

446   The formula allows for obtaining the erosion rate by dividing the distance $D$ between

447   the tree root top and the actual ground surface by the age $A$ of the micromorphology

448   change in root. Because samplings were performed during the summer months, a

449   variable portion of the sampling year (*Year Fraction; YF*) should be added to the $A$

450   parameter for reducing the overestimation of the erosion rate. Hence, the herein

451   applied formula was

452   $$E = D/(A+YF) \qquad (2)$$

453   where

454   $$YF = (1/12) * N° \ month \qquad (3)$$

455   where $N°$ *month* represents the progressive number of the month within a year (e.g.,

456   July = 7; $YF_{July} = 0.583$).

457   Considering that roots from the same tree might be exposed in different times, *Local*

458   *Erosion Rates (LERs)* at single tree root sample and *Average Erosion Rates (AERs)*

459   over long periods in the extended areas (e.g., Bollati et al., 2016a, b) were finally

460   obtained.

461   Besides erosion rates, attention was also paid to the most commonly used

462   dendrogeomorphological indicators for detecting geomorphic disturbance by

463   processes that may trigger erosion (e.g., mass wasting, snow avalanches). These

464   processes in fact may interact with water runoff altering the normal erosion values

465   (Bollati et al., 2016a). The *Compression Wood* (*CW*) is a particular, resistant, and

466   denser kind of wood produced by the tree in response to mechanical stress induced by

467   the tilting of the stem (Fig. 3) caused mainly to creep or other destabilising processes

468   (e.g., Timell, 1986; Bollati et al., 2018). *Traumatic Resin Ducts* (TRDs) are aligned

469   resin ducts, which are specific features that may be produced in trunks affected by

470   traumas deriving from the impact of material caused by geomorphic processes

471 inducing debris transport (e.g., snow avalanches, debris flows, rock falls) (e.g.,

472 Bollschweiler et al., 2008; Garavaglia and Pelfini, 2011). Because TRDs are produced

473 immediately after the stress, they have already been used to date and to discriminate

474 geomorphic processes with a seasonal resolution according to the location of the ducts

475 within the early- or latewood (e.g., Kogelnig-Mayer et al., 2011; Bollati et al., 2018).

476 According to Kogelnig-Mayer et al. (2011), TRDs located within the latewood may

477 indicate, more probably, damages from mass wasting (e.g., debris flows, landslides),

478 which are more frequent during late summer until early autumn; instead TRDs

479 characterising earlywood may indicate, more probably, damages from winter/spring

480 snow avalanches.

481

482 *3.3.    Geopedological sampling and analysis*

483 Soil profiles were chosen for sampling, where possible, in correspondence with

484 specific geomorphic conditions and of dendrogeomorphological sample sites, as

485 described in Table 1. In both study areas, soil profiles were selected (i) along the

486 slope, in order to observe the slope dynamics; (ii) on the edge of gullies, in order to

487 understand the erosion dynamic under water-driven processes; and (iii) in flat and/or

488 stable areas (i.e., undisturbed in Table 1) in order to observe soil development in a

489 steadier geomorphological context. All the profiles were dug taking advantage of the

490 presence of a natural scarp, except for profile SN16/02 where a digger was used. Each

491 soil sample was then subjected to routine laboratory analysis to determine particle size

492 distribution, pH (in 1:2.5 soil:distilled water) and organic carbon content (Walkley-

493 Black method) (Ministero delle Risorse Agricole Alimentari e Forestali, 1994).

494 In regards to the grain - size analyses, air-dried soil samples were treated by wet

495 sieving in order to separate skeleton particles from the fine earth. For what concerns

20

496  fine earth, after a pre-treatment of the samples with $H_2O_2$ (130 volumes), particle size

497  distribution was determined by a combined method consisting of sieving the sand

498  particles (1400–63 μm) and measurement of the silt and clay particles (<63 μm) by

499  aerometry, with the method of the Casagrande aerometer.

500

501  **4. Results**

502

503  *4.1. Multitemporal analysis of gully surface changes caused by water and gravity*

504  *erosion*

505  Concerning the GG site, the main morphometric features are reported in Table 2. The

506  site is quite regularly developed all along its length, but the western edge is less

507  elevated than the eastern edge. The highest difference value (42 m; Table 1) is

508  recorded in the area where the interruption of the eastern edge by the regressive

509  erosion of the external slope occurs.

510  The multitemporal analysis of surface area changes caused by water runoff indicates a

511  general trend of decreasing bare surface areas (Fig. 4, A; Table 1). The percentages of

512  variations with respect to the initial surface area during the 1989-2007 time interval

513  never exceeded 1%. A slight increase (<0.12%) of bare surface is recorded only

514  during the 2007-2012 period. The mapped areas are reported in Fig. 3 as well as the

515  percentage of surface variations, averaged over their respective time interval.

516  Concerning the SN site, water runoff does not homogeneously interest the surface

517  along the main gully, whose width is variable. Three main subsectors can be

518  recognised according to morphometric and gully width observations and

519  measurements (see Table 2):

520  • the main gully is narrower and the edges are regular in the uppermost portion;

21

521    • the main gully is becoming wider and is characterised by a more continuous

522    vegetation coverage on the western side in the central portion; the development of

523    five main *horse-shoe shaped* calanchi basins is evident on the eastern side in the

524    central portion (Fig. 4, B); this sector presents an asymmetric transversal section

525    with a significant difference in altitude between the two scarp edges (60 m; Table 1);

526    and

527    • the last trait is more irregular and asymmetric, as well as well colonised by

528    vegetation and it represents the closure section of the gully.

529    The width variations of the surfaces affected by water runoff at the SN, in the 1988-

530    2006 time interval, is represented by a decrease between 0.11% and 2.46%,

531    accompanied by an increment of vegetation along the calanchi slopes.

532

533    *4.2. Dendrogeomorphological analysis*

534    Concerning trees colonising the surfaces of the GG site, the oldest tree (58 years

535    minimum age) is located along the slope, immediately west of the GG. About half of

536    the trees (40% not considering the trees in the forestry conditions A6 and A7) are 30-

537    40 years old minimum and colonise the slope (mainly A1, A2). Trees belonging to the

538    transects (A5), first mapped in the 2007 orthophoto along the lateral slope of the gully

539    (A5), are younger than 30 years and, more frequently, are <20 years old.

540    Trees with exposed roots are mainly located along the GG scarp edge (A3, A4). The

541    LERs are variable between trees and within the same tree. Along the upper scarp edge

542    (A3), the maximum LER value is 30.57 cm/y, in correspondence with local debris

543    fall. The AER, considering the beginning of the exposure and excluding the minimum

544    and maximum values, is 2.81 cm/y. Also along the slope immediately behind the

545    scarp edge, surface erosion denudates tree roots (Fig. 5). Here, the AER in

22

546    correspondence with the only tree with exposed roots is 0.87 cm/y. The older ages of

547    exposure (1986-2002) are recorded in the lower portion of the scarp (A4). The most

548    recent exposures occur in the upper portion of the scarp (A3), where the maximum

549    LERs have also been calculated.

550    Considering the higher number of trees during recent years, the years with the greatest

551    number of trees characterised by TRDs are 2003 and 2006 followed by 2004, 2007,

552    and 2010 (Fig. 6). During these years, the groups more affected by earlywood and

553    latewood TRDs are A3 and A4. The TRDs in the earlywood are more homogeneously

554    distributed in time and space, particularly along the scarp edge in 2006 and 2007. The

555    latewood TRDs affected A3 trees in 1985, 1990-1992, 1995, and 2008 and affected

556    A5 trees especially in the 2002-2004 time interval.

557    Concerning CW at the GG site, the trend is quite discontinuous. The trees mainly

558    affected are those belonging to the A3 and A4, located on the slope immediately west

559    of the scarp edge and interested continuatively by instability. During the second half

560    of the 1990s of the twentieth century, the CW propagated to the slope trees (A1 and

561    A2).

562    The transects inside the gully (A5) are characterised by abundant CW even if this data

563    should be handled with care as these trees have recently germinated and their young

564    and elastic trunks may be more prone to destabilisation. In general, trees located along

565    the edge are undermined by the instability of the substrate inside the gully, as local

566    falls also involve (besides debris) trees (between 2013 and 2016 evident changes were

567    recorded). The CW is found related, on the inner western slope, to creep and

568    instability induced by the high steepness of the slope itself and of the bottom of the

569    gully.

23

570     Moving to the SN site, tree vegetation in the Gaboè (B1) and in the Montovert area

571     (B2) has been colonising surfaces for a long time but with some differences. The

572     oldest trees were dated to the beginning of the twentieth century by cross-dating mean

573     chronologies from each tree with the reference chronologies; they are located in the

574     western inner part of the geosite (B1.4) and up to the geosite (B1.2) (Fig. 5, B). Trees

575     are not older than 1989 near the bottom of the gully (B1.4), while along the western

576     scarp (B1.3) the oldest tree dated back to 1930. At the B2 site vegetation dated back at

577     least to the end of the 1960s of the twentieth century.

578     Exposed roots were observed and LERs were calculated at the B1.3 (the western scarp

579     edge at the geosite) and at the B2 (Fig. 5, B). In the B1.3 site LERs span between 0.29

580     and 3.01 cm/y. The spatial AER along the scarp edge (B1.3) is 1.38 cm/y. The years

581     of exposure span between 1958 and 2013. In B1.2, located along the Gaboè stream up

582     above the geosite, the LER is 0.29 cm/y. The B2 is characterised by LERs, which are

583     lower between 0.08 and 1.40 cm/y. Exposure years span between 1981 and 2014, and

584     the spatial AER for this period is 0.84 cm/y.

585     The TRD distribution is quite inhomogeneous and less representative than in the GG

586     site. The TRDs are present in B1 during different years within trees. The B1.3 and

587     B1.4 are the subclusters most affected by TRD occurrence. More than one tree is

588     affected by TRDs only during 1999/2000 and 2003/2004. The B1.1 trees in one site

589     present TRDs in 2004/2005. The B2 tree data coincides with the other sites for TRDs

590     only in 2000 and 2004/2005.

591     The CW does not show precise trends and is not abundant as expected. The CW is

592     more frequent in B1.4: in the bottom of the gully and on the eastern slope it is

593     recorded during the period 1990-2005; on the other side it was present before the

594   1990s. An overlapping time interval characterised by CW was also observed for

595   subsites: 1997-2004 for B1.1; 1992-2002 for B2.

596

597   *4.3. Geopedological analysis*

598   The analysed soil profiles at the GG site show a weak degree of development and an

599   unmarked horizon differentiation, except for the soil profile located at the edge of the

600   main gully (P04) and for the soil profile used as a reference and located in the forest

601   (P06).

602   Indeed, soil profiles show thickness <1 m; they are characterised by a moderately

603   expressed soil structure and by granular or subangular blocky aggregates. The colour,

604   in dry condition, is quite homogeneous in overall horizons and profiles (characterised

605   by a hue rarely different from 2.5Y).

606   All soil profiles have a considerable skeleton content (material >2 mm), and gravel is

607   very abundant with peaks over 50% in some horizons (Fig. 7). Gravel content is

608   <10% only in the surficial horizons. In regards to the fine earth, sand is the most

609   represented fraction, which ranges between 17 and 42.6% of the total weight; whereas

610   the less represented grain size fraction is clay, which rarely exceeds 20% of the total

611   weight (Fig. 7).

612   Moreover, grain size distribution cumulative curves (Appendix 1a) show a low degree

613   of selection with a predominant sand presence, except for profiles located in more

614   stable areas (P06 and P08) and for the profile located at the edge of the gully (P04).

615   Generally, the percentages of gravel and sand increase along the profile to the

616   detriment of silt and clay components (Fig. 7). Instead, in profile P07 a little grain size

617   trend anomaly is found: horizon C2 is characterised by a sand, silt, and clay content

618    increase accompanied by a decrease of gravel content when compared to the above

619    horizon (Fig. 7).

620    A decreasing trend with depth of organic carbon is observed in all soil profiles. The

621    absolute quantity of organic carbon varies between 4.1 and 164 g/Kg (Fig. 7).

622    Horizons within the soil profiles have pH values ranging from 5.5 to 7.4 (Fig. 7).

623    Generally, the superficial horizons are more acid, in particular in P03 and P08.

624    The soil profiles studied by geopedological analysis at the SN site (B1), located in a

625    flat and more stable area (SNA16/02; SNA16/03), are more developed and thick when

626    compared to the profiles placed at the edge of gully (SNA16/01 and SN03) or on the

627    slopes (SN01 and SN05). Soil structure is moderately developed and is mainly

628    characterised by granular or subangular blocky aggregates.

629    Particle size distribution in the analysed soil profiles shows that gravel and sand are

630    the most represented grain size fractions (Fig. 8); in fact, sand content varies between

631    16 and 57.4%, and the content of gravel varies between 6.6 and 79.2%. Silt quantity is

632    more variable, instead clay is limited and always below 10% in total weight.

633    Grain size decreases in SN05 and SNA16/03 from the parent material to the surface

634    soil horizons, where the highest clay and silt contents are found.

635    Instead, in SN01, in the deepest horizon 2A there is an increase of silt and clay

636    contents compared to the above horizon. Moreover, the gravel content decreases

637    along the profile, whereas the sand quantity remains roughly constant (Fig. 8).

638    A grain size trend anomaly is also found in SN03, where sand, silt, and clay contents

639    increase in the 2AC horizon, accompanied by a decrease of gravel when compared to

640    the above horizon (Fig. 8).

641    Silt and clay content decreases along the profiles in SNA16/01 and SNA16/02. The

642    coarse material tends to increase, but the superficial horizon shows higher gravel

643   content compared to the below horizon. Moreover, observing the cumulative curves

644   of SNA16/02 grain size distribution (Appendix 1b), the superficial AC horizon shows

645   a very different trend from other horizons. The cumulative curves show a low degree

646   of selection, with a predominant sand presence, except for profiles located in more

647   stable areas (SNA16/02 and SNA16/03).

648   The absolute quantities of organic carbon vary between 3.4 and 101.1 g/Kg (Fig. 8).

649   The organic C values decrease with depth in all the analysed profiles except for SN01

650   and SN03, where the superficial horizon does not have the highest quantities of

651   organic C.

652   In particular, in SN01 the peak of organic C is in the deepest horizon (2A), while in

653   SN03 the organic C content shows a peak in the 2AC horizon (Fig. 8).

654   In all horizons of the analysed soil profiles, the pH values range from 4.1 to 8.1 (Fig.

655   8). On average, the surficial horizons are more acid, in particular in SNA16/02 and

656   SNA16/03. More or less in all profiles the pH increases along the profile, approaching

657   the parent material.

658

659   **5.   Discussion**

660

661   The results obtained in the two study cases allow us for making some remarks on the

662   reliability of applying a multidisciplinary approach to reconstruct slope evolution in

663   relation to geomorphic processes and/or structural setting conditioning on erosion.

664   A summary of the findings at GG and SN is reported in Table 3, where the main

665   indicators of disturbance in both sites are listed.

666   On one side, the sites are very similar concerning climate conditions and bedrock. In

667   the first case, both sites are located along the south-facing slope of a main E-W

27

668    oriented valley, in which climate regime presents a trend characterised by marked

669    drought periods alternating with wet periods, and extreme rainfall events are even

670    more frequent (Frei et al., 1998). This, as in other climate contexts (i.e.,

671    Mediterranean; Della Seta et al., 2009), favours water-related erosion, especially if

672    loose deposits are outcropping. These conditions are also common in other localities

673    where similar measurements on erosion of glacial deposits were performed with the

674    same methodology (e.g., Pyramides d'Euseigne, Valais Canton, Switzerland; Bollati

675    et al., 2017), resulting in lower AERs (0.58 cm/y; Bollati et al., 2017; see discussion

676    after).

677    The sites also present similar bedrocks and, consequently, parent materials as a

678    relevant abundance of ultramafic and calcareous debris was surveyed.

679    Moreover, the multitemporal measurements of the areas affected by erosion allow us

680    for discovering a similar trend between sites. Both sites are characterised by a general

681    reduction of surfaces affected by water runoff, except for the most recent times during

682    which a slight increase was detected at the GG site (0.1%; 2007-2012). All values,

683    considering the possible error using the WMS source, fall within the percentage (i.e.,

684    2%), except for the SN site where during the 1988-1997 time interval the bare surface

685    shows a decrease slightly greater than the plausible error 2% (i.e., 2.46%). Hence, the

686    increase of bare surface could not be interpreted as a significant increase of the areas

687    affected by erosion as expected by other authors (Mortara, 1975).

688    Anyway, in both sites, the maximum LERs have been calculated along the edge of the

689    main gully (30.57 cm/y at GG and 3.01 cm/y at SN). At GG lower values were

690    calculated on the slope surrounding the gully. At SN, even more significant, the AER

691    at B1 (1.32 cm/y, excluding the minimum and maximum values), located along the

692    Punta Leysser DSGSD edge, is greater than AER at B2 (0.90 cm/y, excluding the

28

693 minimum and maximum values), located on the main DSGSD body.

694 Dendrochronological analysis of trees sited along the GG scarp edge shows how the

695 area is locally characterised by debris falls: damaged trees are present in

696 correspondence with the highest values of erosion calculated by means of tree root

697 exposure. This may suggest a more intense deepening of the thalweg that may favour

698 scarp instability. Also at the SN site (B1), local instabilities should be taken into

699 account as documented by ages of trees growing near the bottom of the gully, which

700 were younger (germination year after 1989) and more disturbed.

701 If the surface analysis does not reflect the very local changes along the edges, further

702 multitemporal laser scanner analyses, aimed at detecting variations of the gullies

703 morphology, may be helpful (e.g., Cossart and Fort, 2008).

704 Some significant differences were detected between the sites combining

705 dendrogeomorphological and geopedological results.

706 The more evident difference between the SN and GG sites was detected concerning

707 the recurrence and frequency of the dendrogeomorphological indicators (CW and

708 TRDs). In the GG sites, CW and TRDs are recurrent and provide useful information

709 on the different types of geomorphic events related to surface processes (such as snow

710 avalanches and debris flows), but in SN neither CW nor TRD significant trends were

711 observed. This could be related to the difference in the intensity of surface processes

712 affecting the two investigated slopes. While GG is located along a very steep slope

713 (average steepness at the bottom of the gully is 48%, Table 1) where avalanches are

714 common and vegetation colonises the inner part of the gully with difficulty, SN is

715 located in a less steep area (average steepness at the bottom of the gully is 28.7%,

716 Table 1), being more protected from the geomorphic processes, where vegetation is

717 older and also human impact has been more significant (e.g., reforestation of slopes,

718    human settlements since ancient time in the area). These results suggest one should

719    expect different information coming from dendrogeomorphological indicators

720    according to site local features (e.g., Garavaglia and Pelfini, 2011).

721    Another dissimilarity between sites is related to the maximum LERs that are very

722    different: 30.57 cm/y in the upper portion of the western scarp edge at GG (A3) and

723    3.01 cm/y along the western scarp edge of SN (B1.3).

724    Concerning geopedological results, in the studied soil profiles at GG and SN study

725    sites, the analysis of particle size distribution underlines the preponderant presence of

726    coarse material typical of mountain weakly developed soils. Moreover, the influence

727    of parent material on soil features is also evident taking into consideration the pH

728    analysis, which shows a neutral to slightly alkaline pH in all profiles. Only soil

729    profiles located in stable and flat areas, in the forest (i.e., P06) or outside the Punta

730    Leysser DSGSD area (i.e., SNA 16/02 and SNA16/03), show a good degree of

731    development and are identifiable as *Sols Brunifiés* (Duchaufour, 1995).

732    In fact, in both study sites, the soil profiles located along the slopes (i.e., P01, P02,

733    P03, P07, SN01, and SN05) and at the gully edge (i.e., SNA16/01, SN03, and

734    partially P04) are characterised by a weak degree of development, probably caused by

735    the continuous sedimentation/erosion phases deriving from colluvial events and

736    water-driven erosion.

737    Anyway, the two study sites also show some dissimilarity from a geopedological

738    point of view. The alternation of aggradation/degradation episodes along the slopes

739    are testified only in the SN study site by a buried surface underlined by the presence

740    of grain size discontinuity and by a peak of organic carbon content (i.e., SN03-2AC

741    and SN01-2A horizons); whereas, no buried surfaces are found in the GG study site.

742    Nevertheless, a little grain-size discontinuity is found in P07, probably caused by the

743 incorporation along the profile of coarse material transported by water-driven

744 processes or snow action.

745 Hence, dendrogeomorphological indicators (different response in the two sites) and

746 geopedological techniques (different degree of soil development and

747 presence/absence of buried surface) agree in detecting differences in surface

748 geomorphic processes inducing erosion along slopes in the sites: higher in GG and

749 lower in SN. The application of LERs and AERs allowed both for delineating the

750 local and general trend of erosion.

751 A discussion may be open on the role of geostructural drivers in triggering erosion,

752 combining, hence, the geomorphological and structural conditions characterising the

753 study sites (Fort, 2000; Cossart et al., 2013). The structural conditions may in fact

754 guide, at first, the localisation of the relatively deep incisions along the slopes, prepare

755 a weaker substrate on which erosional processes could easily act, or, again, trigger the

756 erosion rates in relation with Earth surface uplift or lowering. For example, according

757 to different authors (Pini et al., 2013; Forno et al., 2016), the Punta Leysser DSGSD

758 dynamics guided the Quaternary history of the slope in the SN case, in particular, the

759 preservation of Quaternary sediments. Considering, moreover, the asymmetric shape

760 of the SN site (more linear on the western sites and articulated in subbasins along the

761 eastern side), this nonlinearity in erosion patterns may be related to the location of the

762 gully up above the westward diversion of the western edge of the Punta Leysser

763 DSGSD, probably inducing water flow variations. Because, moreover, gully systems

764 are usually characterised by step-like erosional trends, as detected in Mediterranean

765 contexts by Della Seta et al. (2009), these trends may be exasperated by the

766 differential movements especially along the border zones of DSGSDs (Mortara and

767 Sorzana, 1987). As indicated before, the AER along the western scarp of the SN site

31

768    (B1 along the DSGSD edge) is 1.32 cm/y that is slightly higher if compared with the

769    AER on similar deposits in Alpine areas indicated before (i.e., 0.58 cm/y). Also in the

770    GG case, the AER along the scarp edge is higher (2.81 cm/y), with local significant

771    peaks (i.e., 30.57 cm/y). However, if at the SN case the Punta Leysser DSGSD

772    pervasively characterises the slope, there are no signs of a DSGSD surveyed in the

773    GG site by previous authors (Cadoppi et al., 2007). Instead, in the GG case, the slope

774    is very steep and geomorphic processes, related for example to snow action (Sacco,

775    1921; Cadoppi et al., 2002) or gravity (i.e., debris falls), may have contributed

776    significantly to denudation, as demonstrated in other morphoclimatic contexts (Bollati

777    et al., 2016a).

778    These findings are also confirmed by the soil profiles along the GG slope, which are

779    continuously reworked and do not present any buried surface. Moreover, the deep

780    incision, as described before, may be considered a further triggering of scarp

781    instability, linked with the improbable further regressive evolution of the gully,

782    impeded by the presence of the upstream valley shaped in the bedrock (i.e., marble

783    bank of the DM unit herein in structural contact with the SU unit).

784    The results summarised in Table 3 and herein discussed allow us for tracing some

785    final considerations regarding the sites and the related dynamics: (i) AERs are

786    comparable and higher than in other contexts; (ii) denudation processes (e.g., mass

787    wasting, snow avalanches) favoured by a more exposed and steeper slope and testified

788    by the presence of specific indicators, revealed by trees and soils analyses, could be

789    considered more influent in the GG site area, and (iii) since the erosional intensity is

790    similar at the SN site but, at the same time, geomorphic processes responsible for

791    denudation seem currently less active at SN than in the GG area, structural conditions

792   related to DSGSD presence could be invoked as responsible for the similar erosion

793   rates.

794   According to these interpretations, the acquired results contribute to delineation in

795   more detail of the scientific value of the sites and the strengthening of the importance

796   of considering slope evolution in the framework of geoheritage evaluation (e.g.,

797   Bollati et al., 2018). This consideration has fallouts in term of dissemination and

798   educational applications (e.g., Pelfini et al., 2016). In the case of SN, the link with the

799   presence of the Punta Leysser DSGSD is not mentioned in the documentation

800   available for *geosite SN,* but it should be considered relevant for explaining the

801   complexity of interaction between different factors in SN slope evolution. Concerning

802   *geosite GG*, the site was hypothesised to be formed during a single extreme event

803   (Regione Piemonte, 1995) even though no data was provided supporting this

804   hypothesis. No data coming from this investigation supports or contrasts this

805   hypothesis, on the contrary there was evidence of the relevance of a constant action

806   by surface geomorphic processes interacting with the GG evolution. Hence, in the

807   framework of dissemination of physical landscape evolution, it seems appropriate to

808   consider the analysed geosites in the contexts of the respective slope evolution (i.e.,

809   geological, structural, geomorphological drivers). Moreover, their relation with

810   climate trends and vegetation dynamics as ecological indicators of geomorphic

811   activity is relevant (e.g., Bollati et al., 2015; Pelfini et al., 2016; Bollati et al., 2018) as

812   their development cannot be disconnected from their own slope history.

813

814   **6. Conclusions**

815

816   The study sites of Gran Gorgia (GG) and Saint Nicolas (SN) are two gully complex

817   systems developed in glacial deposits on which water-driven processes in relation to

818   local factors (i.e., geological, geomorphological, structural, and climate features) are

819   producing relevant landscapes (i.e., pseudo-badlands feature). Multidisciplinary

820   analyses performed at these sites allowed us for acquiring details on erosional history

821   of the studied slopes. Common and dissimilar traits were detected using trees and

822   soils, and local and average erosion rates were calculated and compared with other

823   morphogenetic and morphoclimatic contexts. The results were discussed and a

824   prevalence of geomorphological constraints on evolution was detected at the GG site,

825   while at the SN site a probable stronger influence of the structural background was

826   considered. The novelty of this work is represented by the multidisciplinary approach

827   used to detect the relationship existing between denudation processes, geological

828   structures, soils and vegetation and their precious roles for analysing applied

829   geomorphology issues. Because the sites have already been classified as geosites by

830   local authorities, their scientific relevance could benefit from the data obtained in the

831   prese,nt research on their genesis, evolution, and local drivers affecting the rates of

832   denudation, connected with the entire slope history. New data, herein presented,

833   represents, moreover, a starting point for Geosciences education.

834

852

853    **References**

854

855    Aigotti, D., Baggio, P., Bois, M.; Cadoppi, P., Costamagna, A. Deline, P., De Renzo,

856        G., Ghelli, A; Giardino, M., Giordan, D., Mortara, G., Nervo, B., Pellegrino, P.,

857        Perotti, L., Riccio, I., Rossato, C., Rossi, C., 2004. I geositi nel paesaggio della

858        Provincia di Torino, Litografia Geda per la Provincia di Torino, Turin, Italy.

859        http://www.provincia.torino.gov.it/territorio/file-

860        storage/download/pdf/dif_suolo/geositi/gran_gorgia.pdf.

861    Alestalo, J., 1971. Dendrochronological interpretation of geomorphic processes.

862        Fennia 105, 140 pp.

863    Alexander, D.E., 1980. I calanchi-accelerated erosion in Italy. Geography 65(2), 95-

864        100.

865  Anselmo, V., Di Nunzio, F., Godone, F., 1975. Torrente (Il) Prebec in territorio di

866      Chianocco (Valle di Susa). Studi ideologici e ricerche storiche. CNR - Laboratorio

867      di Ricerca per la Protezione Idrogeologica nel Bacino Padano, Rapporto interno

868      M.I. 75/1, Turin, 33 pp.

869  Ballantyne, C.K., 2002. A general model of paraglacial landscape response. Holocene

870      12(3), 371-376. https://doi.org/10.1191/0959683602hl553fa.

871  Bollati, I., Leonelli, G., Vezzola, L., Pelfini, M., 2015. The role of ecological value in

872      geomorphosite assessment for the debris-covered Miage Glacier (Western Italian

873      Alps) based on a review of 2.5 centuries of scientific study. Geoheritage 7(2), 119-

874      135. https://doi.org/10.1007/s12371-014-0111-2.

875  Bollati, I., Vergari, F., Del Monte, M., Pelfini, M., 2016a. Multitemporal

876      dendrogeomorphological analysis of slope instability in Upper Orcia Valley

877      (Southern Tuscany, Italy). Geogr. Fis. Din. Quat. 39(2), 105-120.

878      https://doi.org/10.4461/ GFDQ 2016.39.10.

879  Bollati, I., Reynard, E., Palmieri, E.L., Pelfini, M., 2016b. Runoff impact on active

880      geomorphosites in unconsolidated substrate. A comparison between landforms in

881      glacial and marine clay sediments: two case studies from the Swiss Alps and the

882      Italian Apennines. Geoheritage 8(1), 61-75. https://doi.org/10.1007/s12371-015-

883      0161-0.

884  Bollati, I., Pellegrini, M., Reynard, E., Pelfini, M., 2017. Water driven processes and

885      landforms evolution rates in mountain geomorphosites: examples from Swiss Alps.

886      Catena 158, 321-339. https://doi.org/10.1016/j.catena.2017.07.013.

887  Bollati, I, Crosa Lenz, B., Golzio, A., Masseroli, A., 2018. Tree rings as ecological

888      indicator of geomorphic activity in geoheritage studies. Ecol. Ind. 93, 899-916.

889      https://doi.org/10.1016/j.ecolind.2018.05.053.

890    Bollschweiler, M., Stoffel, M., Schneuwly, D.M., Bourqui, K., 2008. Traumatic resin

891        ducts in Larix decidua stems impacted by debris flows. Tree Physiol. 28(2), 255-

892        263. https://doi.org/10.1093/treephys/28.2.255.

893    Brilha, J., 2016. Inventory and quantitative assessment of geosites and geodiversity

894        sites: a review. Geoheritage 8(2), 119-134. https://doi.org/10.1007/s12371-014-

895        0139-3.

896    Burga, C.A., Krüsi, B., Egli, M., Wernli, M., Elsener, S., Ziefle, M., Fischer, T.,

897        Mavris, C., 2010. Plant succession and soil development on the foreland of the

898        Morteratsch glacier (Pontresina, Switzerland): Straight forward or chaotic?. Flora-

899        Morphology, Distribution, Funct. Ecol. Plants 205(9), 561-576.

900        https://doi.org/10.1016/j.flora.2009.10.001.

901    Cadoppi, P., Castelletto, M., Sacchi, R., Baggio, P., Carraro, F., Giraud, V., 2002.

902        Carta Geologica d'Italia alla scala 1:50.000 - Foglio 154, Susa. 1 map, scale

903        1:50000, ISPRA, Rome.

904    Cadoppi, P., Giardino, M., Perrone, G., Tallone, S., 2007. Litho-structural control,

905        morphotectonics, and deep-seated gravitational deformations in the evolution of

906        Alpine relief: a case study in the lower Susa Valley (Italian Western Alps). Quat.

907        Int. 171, 143-159. https://doi.org/10.1016/j.quaint.2006.10.015.

908    Chiarle M., Mortara G., 2001. Esempi di rimodellamento di apparati morenici

909        nell'arco alpino italiano. Suppl. Geogr. Fis. Dinam. Quat. V, 41-54.

910    Chiarle, M., Iannotti, S., Mortara, G., Deline, P., 2007. Recent debris flow

911        occurrences associated with glaciers in the Alps. Global Planet. Change 56(1-2),

912        123-136. https://doi.org/10.1016/j.gloplacha.2006.07.003.

913    Compostella, C., Trombino, L., Caccianiga, M., 2013. Late Holocene soil evolution

914        and treeline fluctuations in the Northern Apennines. Quat. Int. 289, 46-59.

915        https://doi.org/10.1016/j.quaint.2012.02.011.

916    Cossart, E., Fort, M., 2008. Sediment release and storage in early deglaciated areas:

917        towards an application of the exhaustion model from the case of Massif des Écrins

918        (French Alps) since the Little Ice Age. Norw. J. Geogr. 2(2), 115-131.

919        https://doi.org/10.1080/00291950802095145.

920    Cossart, E., Mercier, D., Decaulne, A., Feuillet, T., 2013. An overview of the

921        consequences of paraglacial landsliding on deglaciated mountain slopes: typology,

922        timing and contribution to cascading fluxes. Quaternaire 24(1), 13-24.

923        https://doi.org/10.4000/quaternaire.6444.

924    Cruden, D.M., Hu, X.Q., 1993. Exhaustion and steady state models for predicting

925        landslide hazards in the Canadian Rocky Mountains. Geomorphology 8(4), 279-

926        285. https://doi.org/10.1016/0169-555X(93)90024-V.

927    Curry, A.M., 1999. Paraglacial modification of slope form. Earth Surf. Proc. Land.

928        24(13), 1213-1228. https://doi.org/10.1002/(SICI)1096-

929        9837(199912)24:13<1213::AID-ESP32>3.0.CO;2-B.

930    De Luca, D., Destefanis, E., Forno, M.G., Fratianni, S., Gattiglio, M., Masciocco, L.,

931        Menegon, A., 2009. Studio interdisciplinare per il monitoraggio e la valorizzazione

932        delle sorgenti della valle Susa in previsione di opere a forte impatto ambientale.

933        Memorie Della Società Geografica Italiana 87, 189-199.

934    Della Seta, M., Del Monte, M., Fredi, P., Palmieri, E. L., 2009. Space–time variability

935        of denudation rates at the catchment and hillslope scales on the Tyrrhenian side of

936        Central Italy. Geomorphology 107(3-4), 161-177.

937        https://doi.org/10.1016/j.geomorph.2008.12.004.

938    Duchaufour, P., 1995. Pedology. Soil, vegetation, environment. Ed. 4th, CRC Press,

939        Boca Raton, USA, 274 pp.

940    Eichel, J., Corenblit, D., Dikau, R., 2016. Conditions for feedbacks between

941        geomorphic and vegetation dynamics on lateral moraine slopes: a biogeomorphic

942        feedback window. Earth Surf. Proc. Land. 41(3), 406-419.

943        https://doi.org/10.1002/esp.3859.

944    Farifteh, J., Soeters, R., 2006. Origin of biancane and calanchi in East Aliano,

945        southern Italy. Geomorphology 77(1-2), 142-152.

946        https://doi.org/10.1016/j.geomorph.2005.12.012.

947    Forno, M.G., Gattiglio, M, Gianotti, F., 2012. Geological context of the Becca France

948        historical landslide (Aosta Valley, NW Italy). Alpine and Mediterranean

949        Quaternary 25(2), 125-140.

950    Forno, M.G., Gattiglio, M., Gianotti, F., Guerreschi, A., Raiteri, L., 2013. Deep-

951        seated gravitational slope deformations as possible suitable locations for

952        prehistoric human settlements: an example from the Italian Western Alps. Quat.

953        Int., 303, 180-190. https://doi.org/10.1016/j.quaint.2013.03.033.

954    Forno, M.G., Comina, C., Gattiglio, M., Gianotti, F., Lo Russo, S., Raiteri, L.,

955        Sambuelli L., Taddia, G., 2016. Preservation of Quaternary sediments in DSGSD

956        environments: the Mont Fallère case study (Aosta Valley, NW Italy). Alpine and

957        Mediterranean Quaternary 29(2), 181-191.

958    Fort, M., 2000. Glaciers and mass wasting processes: their influence on the shaping of

959        the Kali Gandaki valley (higher Himalaya of Nepal). Quat. Int. 65, 101-119.

960        https://doi.org/10.1016/S1040-6182(99)00039-7.

961    Frei, C., Schär, C., Lüthi, D., Davies, H.C., 1998. Heavy precipitation processes in a

962        warmer climate. Geophys. Res. Lett. 25(9), 1431-1434.

963        https://doi.org/10.1029/98GL51099.

964    Galeandro, A., Doglioni, A., Guerricchio, A., Simeone, V., 2013. Hydraulic stream

965        network conditioning by a tectonically induced, giant, deep-seated landslide along

966        the front of the Apennine chain (south Italy). Nat. Hazards Earth Sys. 13(5), 1269-

967        1283. https://doi.org/10.5194/nhess-13-1269-2013.

968    Garavaglia, V., Pelfini, M., 2011. The role of border areas for dendrochronological

969        investigations on catastrophic snow avalanches: a case study from the Italian Alps.

970        Catena 87(2), 209-215. https://doi.org/10.1016/j.catena.2011.06.006.

971    Gärtner H., 2007. Tree roots - methodological review and new development in dating

972        and quantifying erosive processes. Geomorphology 86, 243–251.

973        https://doi.org/10.1016/j.geomorph.2006.09.001.

974    Gianotti, F., Forno, M.G., Ivy-Ochs, S., Monegato, G., Pini, R., Ravazzi, C., 2015.

975        Stratigraphy of the Ivrea Morainic Amphitheatre (NW Italy). An updated

976        synthesis. Alpine and Mediterranean Quaternary 28(1), 29-58.

977    Giardino, M., Mortara, G., Chiarle, M., 2017. The glaciers of the Valle d'Aosta and

978        Piemonte regions: records of present and past environmental and climate changes.

979        In: Soldati, M., Marchetti, M. (Eds.), Landscapes and Landforms of Italy, Springer,

980        Cambridge, pp. 77-88.

981    Giordano, E., Giardino, M., Perotti, L., Ghiraldi, L., Palomba, M., 2016. Following

982        the tracks of Charlemagne in the Cottian Alps. The cultural and geological heritage

983        of the Franks Trail (Susa Valley, Piemonte, NW Italy). Geoheritage 8(4), 293-300.

984        https://doi.org/10.1007/s12371-015-0158-8.

985    Guida, D., Pelfini, M., Santilli, M., 2008. Geomorphological and dendrochronological

986       analyses of a complex landslide in the Southern Apennines. Geogr. Ann.: Ser. A,

987       Phys. Geogr. 90(3), 211-226. https://doi.org/10.1111/j.1468-0459.2008.340.x.

988    Hinderer, M., 2001. Late Quaternary denudation of the Alps, valley and lake fillings

989       and modern river loads. Geodin. Acta 14(4), 231-263.

990       https://doi.org/10.1080/09853111.2001.11432446.

991    Holmes, R.L., Adams, R.K., Fritts, H.C., 1986. Tree-ring chronologies of North

992       America: California, Eastern Oregon and Northern Great Basin with procedures

993       used in the chronology development work including user manual for computer

994       program COFECHA and ARSTAN. Chronology Series VI. University of Arizona,

995       Laboratory of Tree-Ring Research, Tucson, USA.

996    Hupp, C.R., Carey, W.P., 1990. Dendrogeomorphic approach to estimating slope

997       retreat, Maxey Flats, Kentucky. Geology 18(7), 658-661.

998    IPLA, 2007. Carta dei suoli del Piemonte, 1 map, 1:250000. S.EL.CA. Ed.

999    Ivy- Ochs, S., Lucchesi, S., Baggio, P., Fioraso, G., Gianotti, F., Monegato, G., Graf,

1000       A., Akçar N., Christl, M., Carraro, F., Forno, M.G., Schlüchter, C., 2018. New

1001       geomorphological and chronological constraints for glacial deposits in the

1002       Rivoli- Avigliana end- moraine system and the lower Susa Valley (Western Alps,

1003       NW Italy). J. Quat. Sci. 33(5), 550-562. https://doi.org/10.1002/jqs.3034.

1004    Keiler, M., Knight, J., Harrison, S., 2010. Climate change and geomorphological

1005       hazards in the Eastern European Alps. Philos. T. Roy. Soc. A. 368(1919), 2461-

1006       2479. https://doi.org/10.1098/rsta.2010.0047.

1007    Kogelnig-Mayer, B., Stoffel, M., Schneuwly-Bollschweiler, M., Hübl, J., Rudolf-

1008       Miklau, F., 2011. Possibilities and limitations of dendrogeomorphic time-series

1009       reconstructions on sites influenced by debris flows and frequent snow avalanche

1010    activity. Arct. Antarct. Alp. Res. 43(4), 649-658. https://doi.org/10.1657/1938-

1011    4246-43.4.649.

1012    Korup, O., 2005. Geomorphic imprint of landslides on alpine river systems, southwest

1013    New Zealand. Earth Surf. Proc. Land. 30(7), 783-800.

1014    https://doi.org/10.1002/esp.1171.

1015    Lucchesi, S., Gianotti, F., Giardino, M., 2015. The Morainic Amphitheatre

1016    Environment: a geosite to rediscover the geological and cultural heritage in the

1017    examples of the Ivrea and Rivoli-Avigliana Morainic Amphitheatres (NW Italy).

1018    In: Lollino G. et al. (Eds.): Engineering geology for society and territory - Volume

1019    8: Preservation of Cultural Heritage, Springer, Cham, pp. 213-216.

1020    https://doi.org/10.1007/978-3-319-09408-3_41.

1021    McColl, S.T., 2012. Paraglacial rock-slope stability. Geomorphology 153, 1-16,

1022    https://doi.org/10.1016/j.geomorph.2012.02.015.

1023    Mercalli, L., Cat Berro, D., Montuschi, S., 2003. Atlante climatico della valle

1024    d'Aosta. Turin, Società Meteorologica Subalpina, 416 pp.

1025    Mercier, D., Étienne, S., Sellier, D., André, M.F., 2009. Paraglacial gullying of

1026    sediment -   mantled slopes: a case study of Colletthøgda, Kongsfjorden area, West

1027    Spitsbergen (Svalbard). Earth Surf. Proc. Land. 34(13), 1772-1789.

1028    https://doi.org/10.1002/esp.1862.

1029    Ministero delle Risorse Agricole Alimentari e Forestali, 1994. Metodi ufficiali di

1030    analisi chimica del suolo, con commenti ed interpretazioni. ISMEA, Roma, 207 pp.

1031    Mortara, G., 1975. Osservazioni preliminari nel bacino del Torrente Prebec (Valle di

1032    Susa). CNR-IRPI Torino Ed., 36 pp.

1033    Mortara, G., Sorzana, P., 1987. Fenomeni di deformazione gravitativa profonda

1034    nell'arco alpino occidentale italiano. Considerazioni litostrutturali e morfologiche,

1035    Boll. Soc. Geol. It. 42, 203-244.

1036    Mortara, G., Turitto, O., 1989. Considerazioni sulla vulnerabilità di alcuni siti adibiti

1037    a campeggio in ambiente alpino. In: Badino V. (Ed.), Suolosottosuolo -

1038    Proceedings of the International Congress on Geoengineering, Litografica Geda,

1039    Turin, 1, 137-144.

1040    Mortara, G., Dutto, F., Godone, F., 1995. Effetti degli eventi alluvionali nell'ambiente

1041    proglaciale. La sovraincisione della morena del Ghiacciaio del Mulinet (Stura di

1042    Valgrande, Alpi Graie). Geogr. Fis. Din. Quat. 18, 295-304.

1043    Panizza, M., 2001. Geomorphosites: concepts, methods and examples of

1044    geomorphological survey. Chinese Sci. Bull. 46(1), 4-5.

1045    https://doi.org/10.1007/BF03187227.

1046    Pelfini, M., Bollati, I., 2014. Landforms and geomorphosites ongoing changes:

1047    concepts and implications for geoheritage promotion. Quaestiones geographicae

1048    33(1), 131-143. https://doi.org/10.2478/quageo-2014-0009.

1049    Pelfini, M., Santilli, M., 2008. Frequency of debris flows and their relation with

1050    precipitation: a case study in the Central Alps, Italy. Geomorphology 101(4), 721-

1051    730. https://doi.org/10.1016/j.geomorph.2008.04.002.

1052    Pelfini, M., Leonelli, G., Trombino, L., Zerboni, A., Bollati, I., Merlini, A., Smiraglia,

1053    C., Diolaiuti, G., 2014. New data on glacier fluctuations during the climatic

1054    transition at~ 4,000 cal. year BP from a buried log in the Forni Glacier forefield

1055    (Italian Alps). Rend. Lin. 25(4), 427-437. doi.org/10.1007/s12210-014-0346-5

1056    Pelfini, M., Bollati, I., Pellegrini, L., Zucali, M., 2016. Earth Sciences on the field:

1057        educational applications for the comprehension of landscape evolution. Rend.

1058        Online Soc. Geol. It., 40, 56-66. https://doi.org/10.3301/ROL.2018.19.

1059    Pini, R., Guerreschi, A., Raiteri, L., Ravazzi, C., 2013. Preistoria degli ambienti d'alta

1060        quota in Valle d'Aosta. Primi risultati di indagini paleobotaniche e archeologiche

1061        sull'altopiano del Monte Fallère. Bull. Et. Preh. Archéol. Alp. 23, 2012-2013.

1062    Polino, R., Bonetto, F.; Carraro, F., Gianotti, F., Gouffon, Y., Malusà, M.G., Martin,

1063        S., Perello, P., Schiavo, A., 2015. Carta Geologica d'Italia. Foglio 90 - Aosta. 1

1064        map, scale 1:50000, ISPRA, Rome.

1065    Régent Instrument Inc., 2001. WinDENDRO 2001. Quebec, Canada

1066    Regione Piemonte, 1995. Atlante Toponomastico del Piemonte Montano - Chianocco,

1067        5. Sottocategoria Toponomastica. Dell'Orso Ed., Torino, 144 pp.

1068    Reynard, E., Fontana, G., Kozlik, L., Scapozza, C., 2007. A method for assessing

1069        "scientific" and "additional values" of geomorphosites. Geogr. Helv. 62(3), 148-

1070        158. https://doi.org/10.5194/gh-62-148-2007.

1071    Rinn, F., 1996. TSAP. Time Series Analysis and Presentation. Version 3.0 Reference

1072        Manual, Heidelberg.

1073    Sacco, F., 1921. Il glacialismo della Valle di Susa. L'universo, 2, 561-592.

1074    Sacco, F., 1927. Il glacialismo nella Valle D'Aosta: memoria del prof. Federico

1075        Sacco. Provveditorato generale dello Stato. Ed. Checchini, Torino, 66 pp.

1076    Smiraglia, C., Azzoni, R.S., D'Agata, C., Maragno, D., Fugazza, D., Diolaiuti, G.A.,

1077        2015. The evolution of the Italian glaciers from the previous data base to the New

1078        Italian Inventory. Preliminary considerations and results. Geogr. Fis. Din. Quat.

1079        38(1), 79-87. https://doi.org/10.4461/GFDQ.2015.38.08.

1080    Stoffel, M., Bollschweiler, M., 2008. Tree – ring analysis in natural hazards research

1081        – an overview. Nat. Hazards Earth Syst. 8, 187–202. https://doi.org/10.5194/nhess-

1082        8-187-2008.

1083    Stoffel, M., Corona, C., Ballesteros-Cánovas, J. A., Bodoque J.M., 2013. Dating and

1084        quantification of erosion processes based on exposed roots. Earth Sci. Rev. 123,

1085        18-34. https://doi.org/10.1016/j.earscirev.2013.04.002.

1086    Timell T. E., 1986. Compression wood in gymnosperms. Springer-Verlag, Berlin, 221

1087        pp.

1088    Tropeano, D., Govi, M., Mortara, G., Turitto, O., Sorzana, P., Negrini, G., Arattano,

1089        M., 1999. Eventi alluvionali e frane nell'Italia Settentrionale (1975 - 1981). IRPI-

1090        CNR Ed., Torino, 280 pp. http://www.irpi.to.cnr.it/documenti/eventi7581.pdf.

1091    Tropeano, D., Luino, F., Turconi, L., 2006. Eventi di piena e frana in Italia

1092        settentrionale nel periodo 2002-2004. IRPI-CNR Ed., Torino, 171 pp.

1093        http://www.irpi.to.cnr.it/documenti/volume20022004.pdf.

1094    Wimbledon, W.A., 1999. GEOSITES - an International Union of Geological Sciences

1095        initiative to conserve our geological heritage. Polish Geological Institute Special

1096        Papers 2, 5- 8.

1097    Zgłobicki, W., Poesen, J., Cohen, M., Del Monte, M., García-Ruiz, J.M., Ionita, I.,

1098        Niacsu, L., Machová, Z., Martín-Duque, J.F., Nadal-Romero, E, Pica, A., Rey, F.,

1099        Solé-Benet, A., Stankoviansky, M., Stolz, C., 2017. The potential of permanent

1100        gullies in Europe as geomorphosites. Geoheritage 1-23. https://doi.

1101        10.1007/s12371-017-0252-1.

**Tables captions list**

**Table 1**

Sampling clusters and subclusters at Gran Gorgia and Saint Nicolas; the geomorphic context is described and the soils profiles and trees codes are indicated, as used in the text

**Table 2**

Morphometric analyses at the study sites: (A) Morphometric measurements of the gullies (AR: altitudinal range, L: bottom length, W: average width, St: steepness; $\Delta$A: altitude difference between edges); (B) Morphometric variations of surfaces affected by water runoff

**Table 3**

Prevailing disturbance indicators at the study areas

Table_1_R2

**Table 1**

Sampling clusters and subclusters at Gran Gorgia and Saint Nicolas; the geomorphic context is described and the soils profiles and trees codes are indicated, as used in the text

| Geomorphic context | GG | | | SN<br>*SN: along the Gaboè stream (B1)*<br>*Rumiod: along the Montovret stream (B2)* | | |
|---|---|---|---|---|---|---|
| | *Soils* | *Trees* | *Notes* | *Soils* | *Trees* | *Notes* |
| Slope | P01<br>P02<br>P03<br>P07 | A1 | steep slope | SN 01<br>SN 05 | B1.1 | steep slope |
| | P08 | A2 | counterscarp | / | / | / |
| Gully edge and peripheral streams | / | A3 | upper W scarp | SN 03 | B1.2 | incipient gully (800 m N); |
| | P04 | A4 | lower W scarp | SNA 16/01<br>/ | B1.3<br>B2 | upper E scarp<br>E scarp |
| Inside the gully | / | A5 | along parallel transects | / | B1.4 | inside the gully |
| Undisturbed (*reference conditions for soils and trees*) | P06 | A6 | within the forest (1.5 km SE; 1300 m a.s.l.); | SNA 16/02<br>SNA 16/03 | / | outside the DSGD |
| | / | A7 | within the forest (1 km SE; 1400 m a.s.l.). | / | B1.5 | within the forest (1.3 km W, 1920 m a.s.l.) |

Table_2_R2

**Table 2**

Morphometric analyses at the study sites: (A) Morphometric measurements of the gullies (AR: altitudinal range, L: bottom length, W: average width, St: steepness; ΔA: altitude difference between edges); (B) Morphometric variations of surfaces affected by water runoff

| (A) Morphometric measurements | | | | | | | |
|---|---|---|---|---|---|---|---|
| | | | AR (m asl) | L (m) | W (m) | S (%) | ΔA (m) |
| GG | | max | 1840 | | | | |
| | | min | 1585 | 530 | 130 | 48.11 | 42 |
| | | range | 255 | | | | |
| SN | | max | 2000 | | | | |
| | | min | 1650 | 1220 | 180 | 28.69 | / |
| | | range | 350 | | | | |
| SN Subtraits | SN_i | max | 2000 | | | | |
| | | min | 1920 | 430 | 170 | 18.60 | 10 |
| | | range | 80 | | | | |
| | SN_ii | max | 1920 | | | | |
| | | min | 1760 | 505 | 276 | 31.68 | 60 |
| | | range | 160 | | | | |
| | SN_iii | max | 1760 | | | | |
| | | min | 1650 | 285 | 93 | 38.60 | < 10 |
| | | range | 110 | | | | |

| | (B) Water runoff affected surface | | | | |
|---|---|---|---|---|---|
| | | 2012 | 2007 | 1998 | 1997 | 1989 |
| **GG** | Area (m²) | 69679.14 | 69261.37 | 72293.47 | 72870.29 | 73492.48 |
| | Variation (m²) | 417.77 | -3032.10 | -576.82 | -622.19 | |
| | *% respect to previous measure* | 0.60 | -4.19 | -0.79 | -0.85 | |
| | Annual average | *83.55* | *-336.90* | *-576.82* | *-77.77* | |
| | *% respect to previous measure* | *0.12* | *-0.47* | *-0.79* | *-0.11* | |
| | Total widening: 2012-2007 | **417.77** | | | | |
| | Annual average | *83.55* | | | | |
| | *% respect to the first measure* | **0.57** | | | | |
| | Total reduction: 2007-1989 | | **-4231.11** | | | |
| | Annual average | | *-235.06* | | | |
| | *% respect to the first measure* | | **-5.76** | | | |
| | | 2012 | 2006 | 1999 | 1997 | 1988 |
| **SN** | Area (m²) | 112967.32 | 121910.18 | 123197.94 | 127120.16 | 163454.70 |
| | Variation (m²) | -8942.86 | -1287.76 | -3922.22 | -36334.54 | |
| | *% respect to previous measure* | -7.34 | -1.05 | -3.09 | -22.23 | |
| | Annual average | *-1490.48* | *-183.97* | *-1961.11* | *-4037.17* | |
| | *% respect to previous measure* | *-1.22* | *-0.15* | *-1.54* | *-2.47* | |
| | Total reduction: 2012-1988 | **-50487.38** | | | | |
| | Annual average | *-2103.64* | | | | |
| | *% respect to the first measure* | **-30.89** | | | | |

**Table_3_R2**

**Table 3**

Prevailing disturbance indicators at the study areas

| | **Relief evolution with related indicators at the study areas** | |
|---|---|---|
| | *Indicators* | *Relevant examples* |
| **GRAN GORGIA** | *CW* | A3, A4, A5 |
| | *TRDs* | A3, A4, A5 |
| | *Relevant erosion rates* | A3, A4 |
| | *Weakly developed soils* | P01, P02, P03 |
| | *Reworked soils with no buried surfaces* | P07 |
| **SAINT NICOLAS** | *Relevant erosion rates different along the DSDG edge and DSDG body* | B1.3, B2 |
| | *Oriented hydrographic pattern* | B1.2; B1.3, B2 |
| | *Weakly developed soils* | SN05, SNA16/01 |
| | *Alternation of aggradation/degradation episodes (i.e., buried surface)* | SN01, SN03 |

**Figures captions list**

**Fig. 1.** Examples of the categories of gully developing on glacial deposits in the mountain environment. (A) Breach in the moraines primarily related to LIA and, secondarily, to the1920-1921 glacier advance at the Southern Mulinet Glacier in the Stura di Lanzo Valley (category 1 along the text); (B) Gran Gorgia deep gully cut in the upper Pleistocene glacial deposits along the northern flank of the lower Susa Valley (category 3 along the text); (C) Saint Nicolas calanchi, incised in glacial and fluvioglacial deposits on the northern side of the Aosta Valley (category 2 along the text). The satellite images used for each site are courtesy of ESRI, Digital Globe, GeoEye, earthstar Geographics, CNES Airbus DS, USDA, USGS, AeroGRID, IGN, and the GIS User Community.

**Fig. 2.** Iconography (upper and lower portion) and location of the study sites in northwestern Italy (in the middle). The locations of the Ivrea and the Rivoli-Avigliana morainic amphitheatres is reported as a reference of the Pleistocene maximum advance. The reaches of the Aosta and Susa valleys located between the study sites and the Pleistocene moraine amphitheatres are indicated in yellow. site A - Gran Gorgia: photo by G. Volpi, 2013; Site B1 - Saint Nicolas and B2 - Rumiod: photo by M. Pellegrini, 2016.

**Fig. 3.** Three examples of exposure year determination on roots from *Larix decidua* Mill. at GG site. In the low-right portion of the figure, a tilted stem inside the SN main gully is reported.

**Fig. 4.** Morphometric analysis on bare surface variations through time using orthophotos freely available through the Web Map Services (WMS) of the Geoportale Nazionale (http://www.pcn.minambiente.it/PCNDYN/catalogowms.jsp?lan=it). (A) Gran Gorgia; (B) Saint
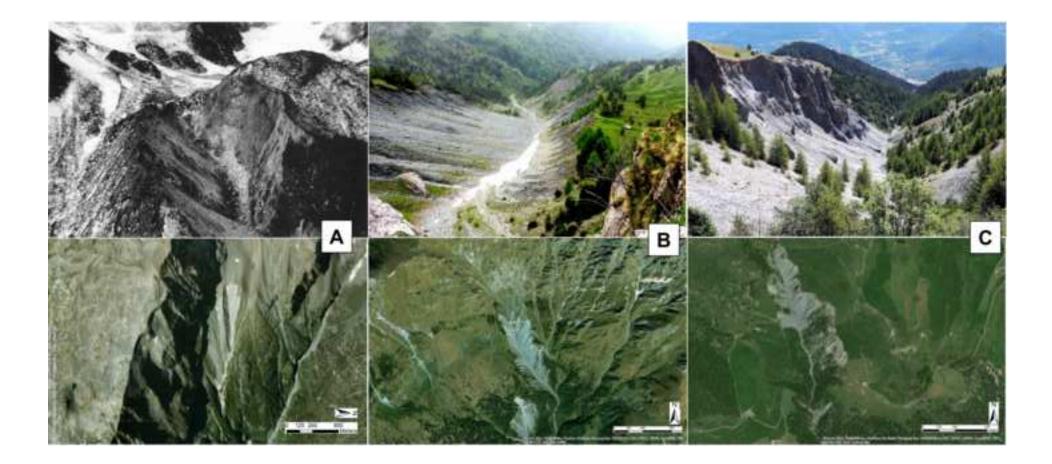
Nicolas. In the middle, the graph of absolute surface variation (above) and of the percentages of average area variation related to their time interval (below).
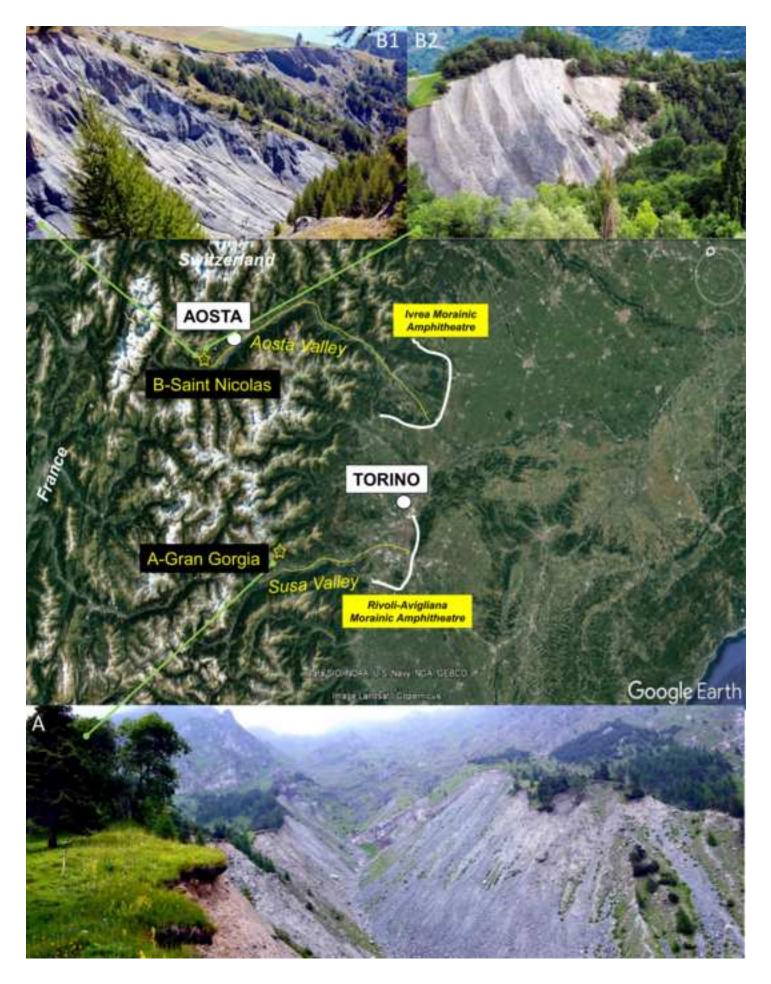
**Fig. 5.** Local erosion rates (LERs) at the Gran Gorgia (A), Saint Nicolas (B1), and Rumiod (B2) samples clusters and subclusters. The indicated values are expressed in cm/y with the related year of exposure. The background images are three-dimensional prospects generated using Google Earth Pro 2017.

**Fig. 6.** Graphs showing the relation between TRDs (distinguishing between early, and latewood) and the number of trees (A) and between TRDs, CW and number of trees for the Gran Gorgia study site. In (B) the trees affected by TRDs and CW are expressed in percentage in respect to the trees germinated in that year. The 2014 and 2015 values are lower because of the lower number of trees added to the clusters during the second field campaign in 2016.
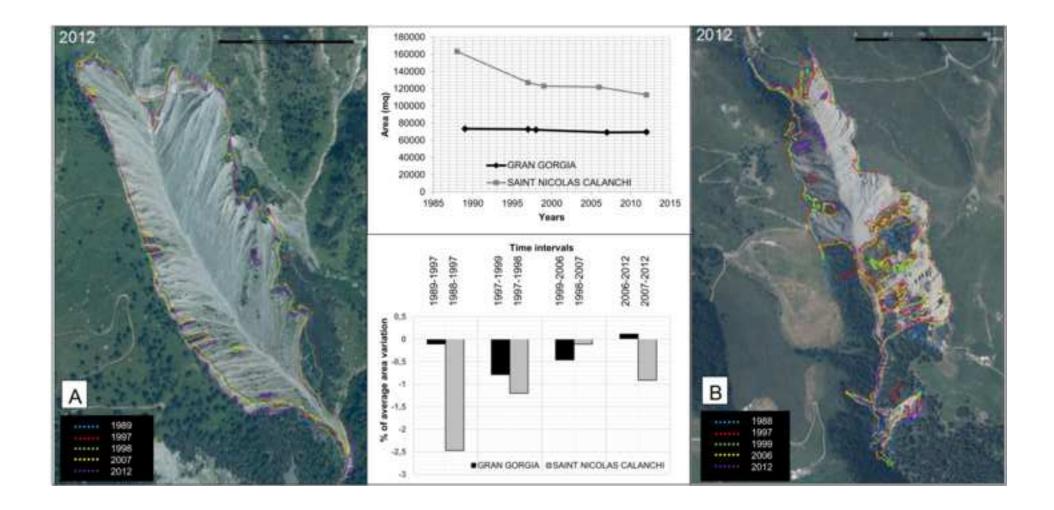
**Fig. 7.** Particle size distribution, organic C content, and pH values in the studied profiles of the Gran Gorgia study area. Particle size distribution plot: the gravel content is depicted in black, the sand content is depicted in dark grey the silt content is depicted in grey and the clay content is depicted in light grey. Only the gravel content data is available in horizons P01 OA, P02 O, P02 AC1, P02 AC2, P03 O, P06 O, and P08 AC2.
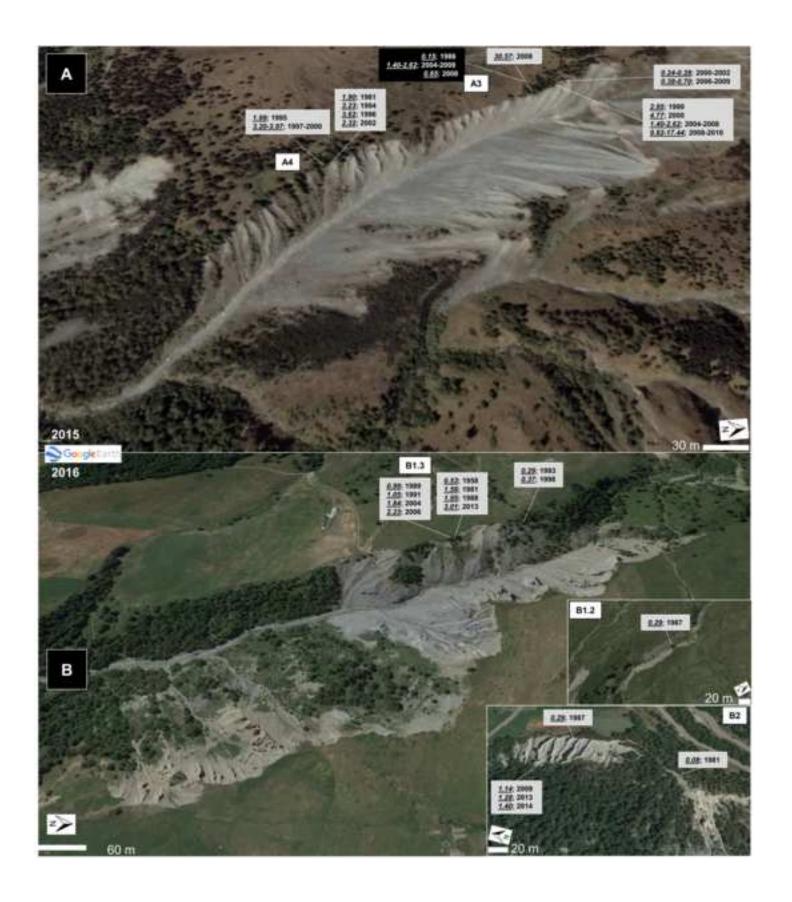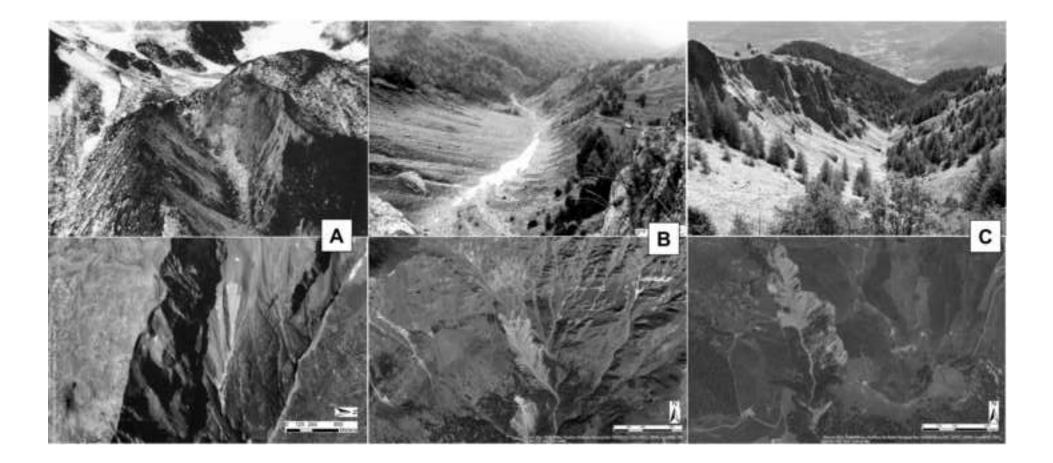
**Fig. 8.** Particle size distribution, organic C content, and pH values in the studied profiles of the Saint Nicolas study area. Particle size distribution plot: the gravel content is depicted in black, the sand content is depicted in dark grey, the silt content is depicted in grey, and the clay content is depicted in light grey.
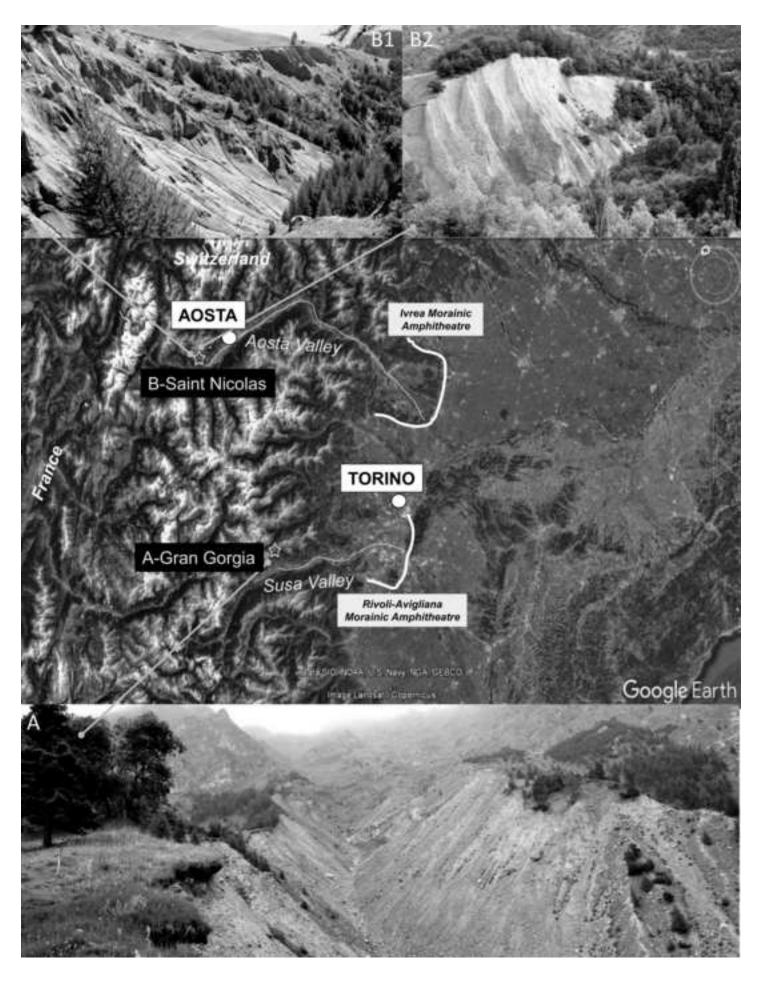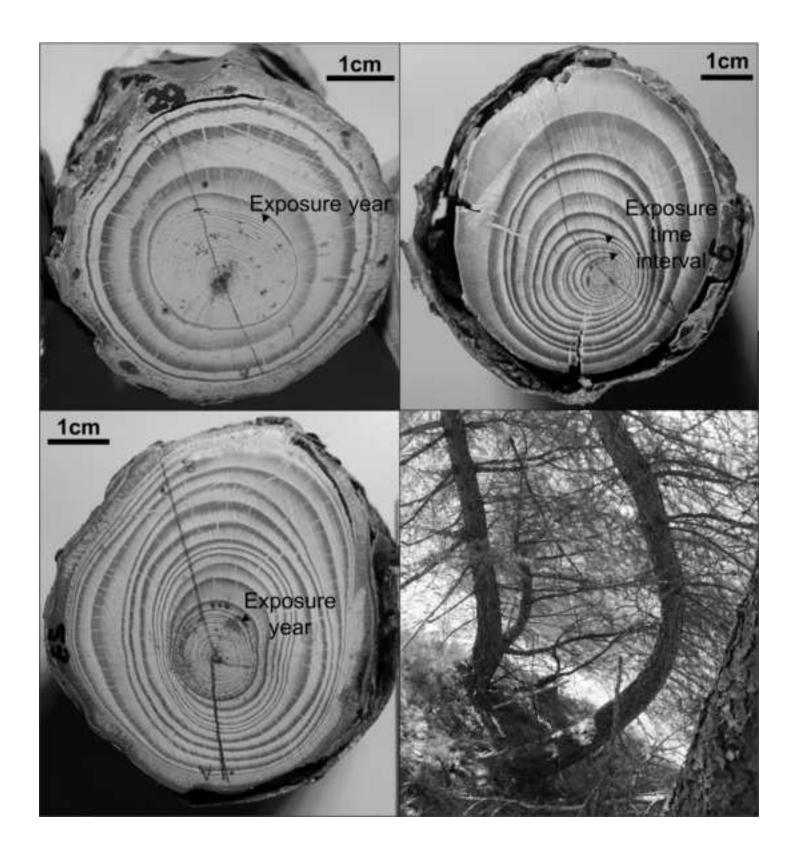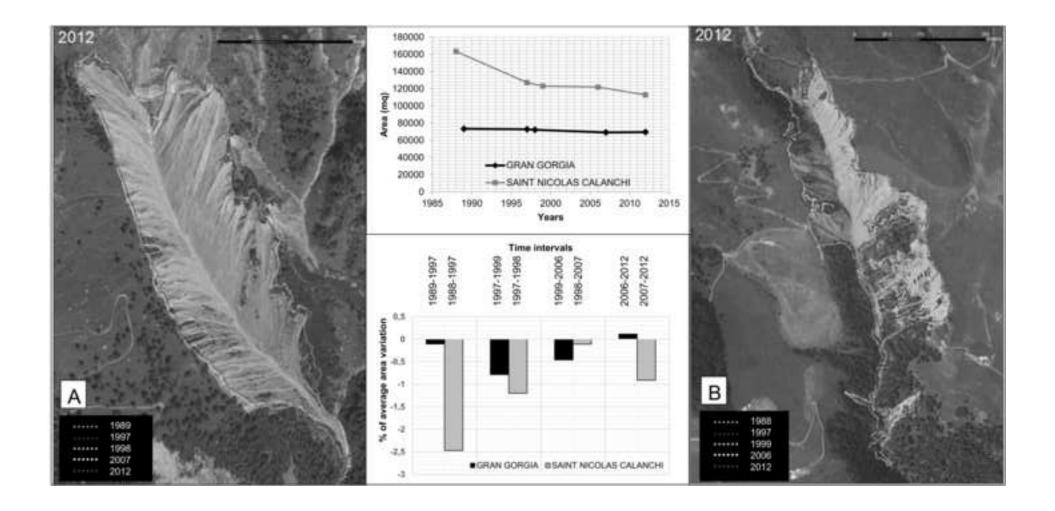
Particles size distribution — Organic C content (g/Kg) — pH

| Profile / Horizon | pH |
|---|---|
| **P01** | |
| OA (0-10 cm) | 6.0 |
| A (10-18 cm) | 6.2 |
| AC1 (18-25 cm) | 6.1 |
| AC2 (25-33 cm) | 6.2 |
| AC3 (33-38+ cm) | 6.1 |
| **P02** | |
| O (0-8 cm) | 6.4 |
| A (8-19 cm) | 6.5 |
| AB (19-27 cm) | 6.8 |
| AC1 (27-33 cm) | 7.0 |
| AC2 (33-38+ cm) | 7.3 |
| **P03** | |
| O (0-5 cm) | 5.7 |
| A (5-14 cm) | 5.5 |
| AB1 (14-23 cm) | 5.9 |
| AB2 (23-30 cm) | 5.8 |
| AC (30-40+ cm) | 5.8 |
| **P04** | |
| O (0-10 cm) | 6.5 |
| A (10-20 cm) | 6.7 |
| AC (20-30 cm) | 6.9 |
| C1 (30-40 cm) | 7.4 |
| C2 (40-50 cm) | 6.6 |
| C3 (50-65+ cm) | 6.8 |
| **P06** | |
| O (0-1 cm) | 5.9 |
| A (1-8 cm) | 6.0 |
| AB1 (8-25 cm) | 6.1 |
| AB2 (25-42 cm) | 6.0 |
| B1 (42-55 cm) | 6.0 |
| B2 (55-70 cm) | 6.4 |
| BC1 (70-80 cm) | 6.5 |
| BC2 (80-85+ cm) | 6.5 |
| **P07** | |
| AO (0-10 cm) | 5.9 |
| AC (10-25 cm) | 6.9 |
| C1 (25-45 cm) | 6.8 |
| C2 (45-55 cm) | 6.7 |
| C3 (55-75+ cm) | 6.8 |
| **P08** | |
| A (0-15 cm) | 5.7 |
| AC1 (15-25 cm) | 5.5 |
| AC2 (25-30+ cm) | 5.6 |

**Interactive Map file (.kml or .kmz)_R1**
**Click here to download Interactive Map file (.kml or .kmz): Study_Sites_Location_R1.kml**

**Appendix_1**

Click here to download Supplementary material for online publication only: Appendix 1.pdf